Petroleum Open File Report POF 10 - 90

Evaluation of the Lower Amaranth Formation in the South Pierson Field, Southwestern Manitoba

by M. Arbez

Hon. Harold J. Neufeld
Minister

Ian Haugh
Deputy Minister

H. Clare Moster
Assistant Deputy Minister

L.R. Dubreuil
Director, Petroleum Branch

Manitoba
Energy and Mines
Petroleum

1990

91-07154/

TABLE OF CONTENTS

Abstract 2
Introduction 2
Availability of Data 2
Methodology 2
A) Porosity 2
1) Total Porosity from Neutron-Density Log 2
2) Total Porosity from Sonic Log 3
3) Effective Porosity from Neutron-Density Log 3
B) Permeability 3
C) Clay Volume 3
D) Cation Exchange Capacity 4
E) Formation Water Resistivity 4
F) Formation Factor 4
G) Water Saturation 5
1) Sw from Waxman-Smits Model (Sww) 5
2) Sw from Dual Water Model (Swd) . . 6
3) Electromagnetic Propagation "CRIM" (Swept or Sxo) 6
4) Quick-look Sw 6
Sw Results 6
Lower Amaranth Pool Descriptions 7
Production Decline and Recovery Factors . . . 7
A) South Pierson Lower Amaranth A Pool . 7
B) South Pierson Lower Amaranth B Pool . 8
Oil Production and Oil-in-Place 8
A) Underachievers 8
B) Overachievers 8
Future Lower Amaranth Pool Development . . 9
A) Recompletions 9
B) Drilling Locations 9
1) A Pool 9
2) B Pool 9
3) C Pool 9
Conclusions 9
Recommendations 10
References 10
Appendix A: Nomenclature 11
Appendix B: South Pierson Lower Amaranth Formation Water Resistivities . . 12
Appendix C: Electromagnetic Propagation "CRIM" 12
Appendix D: South Pierson Lower Amaranth Petrophysical Calculations . . . 13

Tables

Table 1: Reservoir Engineering Properties of the Lower Amaranth Formation 21
Table 2: Lower Amaranth Recompletion Candidates 22
Table 3: Lower Amaranth Drilling Candidates 23

Figures

Figure 1: Study Area 24
Figure 2: Type Log of Lower Amaranth Formation- Home Scurry S. Pierson 4-1-2-29 WPM 25
Figure 3: Neutron-Density Porosity Crossplot 26
Figure 4: Core Total Porosity versus Sonic Travel Time 27
Figure 5: CEC versus (1-Adsorbed Water Index) 28
Figure 6: Formation Factor versus Total Porosity 29
Figure 7: Swept versus Waxman-SmitsSw 30
Figure 8: Waxman-Smits Sw versus Archie Sw 31
Figure 9: Lower Amaranth Formation-South Pierson Field Original Oil-in-Place per Unit Area Map 32
Figure 10: Production History for 9-24-2-29 WPM South Pierson Lower Amaranth A Pool 33
Figure 11: Production History for South Pierson Lower Amaranth B Pool (4 wells) 34
Figure 12: Original Oil-in-Place per Unit Area versus Oil Production 35
Figure 13: Production History for 12-30-2-28 WPM - South Pierson Lower Amaranth A Pool 36

ABSTRACT

Conventional log analysis techniques fail to yield reliable porosities and water saturations for the clay-bearing Lower Amaranth Formation in the South Pierson study area in southwestern Manitoba (Figure 1). This petrophysical study presents a method to obtain effective and total porosities and water saturations for this formation. Simple water saturation equations have been developed to match results from more complex techniques to permit reliable quick-look water saturations to be obtained for the Lower Amaranth Formation in the South Pierson Field.

INTRODUCTION

The South Pierson Field is located in Townships 1 and 2, Ranges 28 and 29 WPM in southwestern Manitoba (Figure 1). Nearly 60% of the cumulative oil production and 80% of the current oil production from the field is obtained from the Lower Sandy Member of the Lower Amaranth Formation. The Mississippian Mission Canyon Formation is also productive in the South Pierson Field.

A type log of the Lower Sandy Member is shown in Figure 2. The Lower Sandy Member unconformably overlies the Mississippian and consists of siltstones with stringers of mudstone interbedded with fine to medium-grained sandstones.

In 1981, the Lyleton Corporation reportedly discovered the South Pierson Lower Amaranth A Pool (the A Pool) with the completion of Lyleton et al S. Pierson 12-30-2-28 WPM. However, as discussed later in the report, there is some doubt as to whether the underlying Mission Canyon Formation was partially or wholly contributing to the production of oil in this well. The well Lyleton et al S. Pierson 9-24-2-29 WPM, which was completed in 1982, may be the actual discovery well for the A Pool.

In 1985, Home Oil Company Limited discovered the South Pierson Lower Amaranth B Pool (the B Pool) with the completion of Home et al S. Pierson 16-8-2-29 WPM. The B Pool accounts for 90% of the current oil production from the Lower Amaranth Formation in the South Pierson Field.

Three other small Lower Amaranth pools have also been designated in the South Pierson Field.

Because of the low permeabilities encountered in the Lower Amaranth Formation, all but one of the Lower Amaranth producers have been fractured.[1]

This study presents a method of calculating porosities and water saturations for the Lower Amaranth Formation in the South Pierson Field.

Oil-in-place and remaining reserve estimates are made for all designated Lower Amaranth pools in the field.

AVAILABILITY OF DATA

The Lower Amaranth Formation has been extensively logged and cored in the South Pierson Field. Analyses of conventionally-dried core are available for most Lower Amaranth producers. In addition, analyses of humidity-dried cores are available for four wells; 6-7-2-29 WPM, 16-8-2-29 WPM, 16-10-2-29 WPM and 4-21-2-29 WPM.

The quick-drying conditions of a conventional oven drive off clay-bound water. Therefore cores dried in this manner can be analysed to determine total porosity. The slow, humidity-controlled drying conditions of a humidity oven result in the retention of clay-bound water and permit the determination of effective porosities.

The Lower Amaranth cores for 8-10-2-29 WPM and 6-19-2-29 WPM have been petrographically analysed. The mineralogy and clay percentages for the 6-19-2-29 WPM core are available through X-ray diffraction (XRD).[2,3]

A relatively large number of analyses of Lower Amaranth formation water are available in the study area. Formation water resistivities (R_W) from these analyses are used in several saturation models to obtain reliable water saturations.

Because of the large amount of petrophysical data available, it is possible to conduct an extensive formation evaluation of the Lower Amaranth in the study area.

The nomenclature used in this report is listed in Appendix A.

METHODOLOGY

A) Porosity

1) Total Porosity from Neutron-Density Log

Porosities from conventionally-dried core samples represent total porosities (Φ_T). Figure 3 is a density porosity (Φ_D) versus neutron porosity (Φ_N) crossplot (sandstone scale on logs). The 45 degree theoretical clean sand line ($\Phi_D = \Phi_N$) can be used for porosity determination in the Lower

Amaranth sand. When the Lower Amaranth sand is clean, the density and neutron porosity log traces are assumed to track together.

The following procedure[4] is used to develop a neutron-density total porosity crossplot for the Lower Amaranth in the study area:

1) depth-shift Φ_T from core to match Φ_D and Φ_N log traces
2) read Φ_D and Φ_N over a log interval showing consistent porosities; plot this sample point on the neutron-density crossplot (point T)
3) locate the corresponding Φ_T from the core sample and plot along clean sand line (point T′)
4) join T′ to T with a straight line
5) calculate the slope of the T′ - T line.

Step (5) gives the slope of a line along which Φ_T does not vary.

The preceding procedure was repeated for a number of sample points in the study area. The following equation is the most commonly observed core to log total porosity relationship:

$$\Phi_T = \frac{(0.52\,\Phi_N + \Phi_D)}{1.52} \qquad ...(1)$$

Φ in percentage, sandstone scale

Equation (1) is graphically shown in Figure 3.

2) Total Porosity from Sonic Log

Sonic waves travel through both reservoir rock and fluid-filled pore space.

Sonic log traces were depth-shifted to match core total porosity traces in the study area and the following sonic log to core total porosity relationship was derived:

$$\Phi_T = 0.19\,\Delta t - 37.1 \qquad ...(2)$$

Φ in percentage

Δt is travel time in µsec/metre

Equation (2) is graphically shown in Figure 4.

If Φ_T is set to zero in Equation (2), the corresponding Δt represents the matrix travel time (Δt_{ma}). Typically, Δt_{ma} ranges from 167 to 182 µsec/metre for sandstones[5]. The Lower Amaranth Δt_{ma} from Equation (2) is 195 µsec/metre.

If Φ_T is set to 100% in Equation (2), the corresponding Δt represents the fluid travel time or Δt_{fl}. Typically, Δt_{fl} = 623µsec/metre.[5] The value for Δt_{fl} from Equation (2) is 722 µsec/metre.

The values of Δt_{ma} and Δt_{fl} for the Lower Amaranth are slightly outside the range of values typically encountered in the literature but are considered reasonable.

3) Effective Porosity from Neutron-Density Log

Porosities from humidity-dried core samples represent effective porosities (Φ_e).

The procedure described in Section A-(1) was followed, this time using core effective porosities (E′-E line). The following equation is the most commonly observed core to log effective porosity relationship:

$$\Phi e = \frac{(0.16\Phi_N + \Phi_D)}{1.16} \qquad ...(3)$$

Φ in percentage, sandstone scale

Equation (3) is graphically shown in Figure 3.

B) Permeability

No correlation between Lower Amaranth core permeability and porosity or clay volume could be determined in the study area. Because of this, no quantitative analysis has been conducted on permeability data in this report.

C) Clay Volume

Evaluation of clay content in the Lower Amaranth is important for two reasons:

1) to evaluate reservoir quality, and
2) to correlate clay volume (V_{CLAY}) to cation exchange capacity (*CEC*), to estimate more accurate water saturations.

Reservoir quality increases as V_{CLAY} decreases. As V_{CLAY} decreases the effective porosity of the formation increases and clay swelling problems are reduced.

An XRD study(3) conducted on samples from 6-19-2-29 WPM shows that chlorite and illite are the two most common clay minerals in the Lower Amaranth.

A correlation between V_{CLAY} (XRD) and the separation between Φ_N and Φ_D was obtained for 6-19-2-29 WPM:

$$V_{CLAY} = .093 \times 10^{0.134(\Phi_N - \Phi_D)} \qquad ...(4)$$

Φ in percentage, sandstone scale

V_{CLAY} in percentage

Equation (4) yields $V_{CLAY} = 0.1\%$ along the clean sand line ($\Phi_D = \Phi_N$) in Figure 3. This is a remarkably good match and lends credence to the Φ_D versus Φ_N crossplot.

A correlation between V_{CLAY} (XRD) and the gamma ray was also obtained for 6-19-2-29 WPM.

$$V_{CLAY} = 0.63(GR) - 23.23 \quad ...(5)$$

GR is the gamma ray reading (API)

V_{CLAY} in percentage

Equation (5) indicates that a gamma ray reading of 36.9 API units is representative of a clean sand and a reading of 195.6 API units represents 100% clay.

D) Cation Exchange Capacity

The cation exchange capacity (*CEC*) of a clay mineral is a measure of the concentration of cations residing on the mineral surface. The *CEC* varies with the type and volume of clays present.

The suppression of resistivity by water-bearing clays is a function of the *CEC* of those clays. Shaly sand water saturation models, which will be discussed later in the report, require accurate *CEC* data. It is important to know the types and percentages of clays present in the Lower Amaranth so that a correlation between V_{CLAY} and *CEC* can be derived.

As noted, four Lower Amaranth cores have been analysed after both humidity and conventional drying. By calculating the unhumidified dry weight of conventionally-dried samples and the humidified dry weight of humidity-dried samples, the Adsorbed Water Index (*AWI*) can be calculated.

The *AWI* is defined in formation evaluation literature:[6]

$$AWI = \frac{unhumidified\ dry\ weight}{humidified\ dry\ weight}$$

An empirical relationship between *CEC* and *AWI* is available in the literature and is shown on Figure 5[6]. The *AWI* for every core sample for the four wells was determined and Figure 5 used to calculate a corresponding *CEC* for the sample. The following equations relate *CEC* to V_{CLAY} in the Lower Amaranth:

$$CEC = 0.37V_{CLAY} + 7.15 \quad ...(6)$$

V_{CLAY} derived from Equation (4)

$$CEC = 0.43V_{CLAY} + 2.42 \quad ...(7)$$

V_{CLAY} derived from Equation (5)

$$CEC = 0.46V_{CLAY} + 3.78 \quad ...(8)$$

V_{CLAY} is the average from Equations (4) and (5)

V_{CLAY} in percentage

CEC in *meq*/100g

E) Formation Water Resistivity

Accurate formation water resistivities (R_W) are required to calculate water saturations from resistivity logs. Wellhead water sample resistivities have been measured for several Lower Amaranth producers in the study area. Temperature-corrected R_W values range from 0.038 to 0.061 ohm-metres and average 0.040 ohm-metres (see Appendix B).

F) Formation Factor

The formation factor (F) is a key variable used to determine water saturations. By definition:

$$F = \frac{R_O}{R_W}$$

where R_O is the wet formation resistivity

Typically, formations exhibit a log to log correlation between F and Φ_T. For wet Lower Amaranth intervals, the following correlation is observed and is graphically shown in Figure 6:

$$F = \frac{0.62}{\Phi_T^{\ 1.59}} \quad ...(9)$$

The Archie equation is a commonly-used water saturation equation. It defines the formation factor as follows:

$$F = \frac{a}{\Phi_T^{\ m}}$$

where:

a is the formation factor when $\Phi_T = 100\%$

m is the cementation factor or the slope of an F versus Φ_T plot.

From Equation (9), the coefficient a or F at $\Phi_T = 100\%$ is 0.62. The coefficient m or the slope of the F versus Φ_T line is 1.59.

Many factors affect the coefficients a and m. Normally, a for a sandstone ranges from 0.62 (Humble formula) to 1.0 (Archie equation).

The coefficient m is a function of the degree of cementation, rock wettability, pore network tortuosity and grain-size distribution. The cementation factor usually ranges from 1.3 to 2.2. Generally, m increases as the fluid path in the pore network becomes more tortuous. The cementation factor is generally lower in water-wet rock than in oil-wet rock. The cementation factor also increases with the degree of consolidation of the formation. A cementation factor of 1.59 for the Lower Amaranth is relatively low, but does fall within the acceptable range discussed in the literature.[7]

G) Water Saturation

Four different water saturation methods were used to evaluate the Lower Amaranth in the study area:

1) Waxman-Smits model,
2) Dual Water model,
3) electromagnetic propagation complex refractive index method or "CRIM", and
4) quick-look Sw equation.

The first three methods are complex empirical solutions which are best suited to computer application. The theory behind these methods is beyond the scope of this study and will not be discussed in great detail.[4]

The Waxman-Smits and Dual Water methods are empirically-derived models which are designed to calculate water saturations (Sw) for clay-bearing sands.

The electromagnetic propagation tool (EPT) is a shallow reading open hole device which emits electromagnetic waves into the formation and measures the attenuation and propagation of these waves at a receiver. The dielectric permitivity (ε) of a formation is a function of both attenuation and propagation times and can be used to estimate Sxo (Sw near the wellbore). The dielectric permitivity is not significantly affected by water salinity as are resistivity measurements. Dielectric permitivity is a function of the water-filled porosity. The electromagnetic propagation "CRIM" method is a set of complex equations which are iteratively solved to determine Sxo.

An empirical equation in the form of the Archie equation has been developed for the Lower Amaranth in the study area. It is a reliable quick look method of making Sw estimates.

1) Sw from Waxman-Smits Model (Sww)

The Waxman-Smits equation[4] can be written as follows:

$$C_t = \frac{C_w S_{ww}^{\,n}}{F^*} + \frac{B Q_v S_{ww}^{\,n-1}}{F^*} \qquad ...(10)$$

The coefficient n is the saturation exponent. Special core analysis work conducted on the Lower Amaranth Formation in the Waskada Field[8] determined that n=2. If n is set to 2, Equation (10) becomes a simple quadratic:

$$X = \frac{-b \pm (b^2 - 4ac)^{1/2}}{2a} \qquad ...(11)$$

where :

$a = C_w / F^*$

$b = BQ_v / F^*$

$c = -C_t$

$X = S_{ww}$

All of these parameters are described in Appendix A and are briefly defined here:

$C_w = 1/R_w$

$C_t = 1/R_t$

$$B = \frac{-1.28 + .225T - .0004059T^2}{1 + R_w^{\,1.23}(0.045T - .27)}$$

$$Q_v = \frac{CEC\,(1 - \Phi_T)\,\rho ma}{\Phi_T}$$

$F^* = F\,(1 + R_w B Q_V)$

CEC in meq/gram, ρma from density log

Temperature in degrees C

R_t from deep resistivity log trace

F obtained from Equation (9)

2) Sw from Dual Water Model (*SWD*)

The Dual Water equation[4] can be written as follows:

$$C_t = \frac{C_W S_{WD}^{n}}{F_0} + \frac{S_{Wb}(C_{CW} - C_W) S_{WD}^{n-1}}{F_0}$$

...(12)

If n is set to 2 (see section G-(1)), Equation (12) becomes a simple quadratic:

$$X = \frac{-b \pm (b^2 - 4ac)^{1/2}}{2a} \quad ...(13)$$

where:

$a = C_w / F_O$

$b = S_{Wb}(C_{CW} - C_W) / F_O$

$c = - C_t$

$X = S_{WD}$

All of these parameters are described in Appendix A and some have been previously defined in section G-(1). New parameters are briefly defined here:

$$S_{Wb} = \frac{\Phi_{Wb}}{\Phi_T}$$

$$\Phi_{Wb} = \Phi_T - \Phi_e$$

$$C_{CW} = \frac{\beta Q_V}{\Phi_{Wb}}$$

$$\beta = \frac{2.05\,(T + 8.5)}{30.5}$$ Temperature in degrees C

$$F_0 = F^* (1 - V_{qh} Q_V)$$

$$F^* = F (1 + R_W B Q_V)$$

$$V_{qh} = \frac{96}{(T_K + 298)}$$ Temperature in degrees K

3) Electromagnetic Propagation "CRIM" (*SWEPT* or *SXO*)

The "CRIM" method of calculating S_{xo} involves a set of equations which are iteratively solved to obtain the water-filled porosity (Φ_{EPT}) and the resistivity of the mud filtrate (R_{mf}).

S_{xo} is then determined by the equation $S_{xo} = \frac{\Phi_{EPT}}{\Phi_T}$.

The "CRIM" method is described in detail in Appendix C.

4) Quick-Look *Sw*

The previous water saturation interpretation techniques are complex and require computer assistance. It is necessary to develop a reliable quick-look method of calculating S_W.

The basic Archie equation is:

$$S_W{}^{n} = \frac{aR_W}{\Phi^m R_t} \quad ...(14)$$

As illustrated earlier, n=2, a=0.62 and m=1.59 for the Lower Amaranth Formation in the study area. Substituting these values in Equation (14), we get:

$$S_W{}^{2} = \frac{0.62 R_W}{\Phi_T{}^{1.59} R_t} \quad ...(15)$$

Sw RESULTS

Appendix D lists S_{WW}, S_{WD}, S_{WEPT} or S_{XO} and Archie S_W results for the Lower Amaranth in the study area.

The following equation is derived from a crossplot of Waxman-Smits water saturations and Dual Water saturations. It shows that S_{WW} is consistently 20 percentage points lower than S_{WD}.

$$S_{WW} = 1.04 S_{WD} - 21.7 \quad ...(16)$$

S_W in percentage

Figure 7 is a S_{WEPT} versus S_{WW} crossplot. S_{WEPT} or S_{XO} values are generally equal to or greater than S_{WW}. This may indicate that S_{WEPT} matches S_{WW} when little or no oil flushing occurs near the wellbore and S_{WEPT} is greater than S_{WW} when oil flushing occurs. $R_{mf\ EPT}$ values calculated by the "CRIM" method average between 0.02 and 0.03 ohm-metres, which are relatively close to the temperature-corrected field average for R_W of 0.04 ohm-metres. This indicates there is a lack of oil flushing near the wellbore in the Lower Amaranth.

S_{WEPT} or S_{XO} values are consistently less than S_{WD}. This appears to indicate that S_{WD} is consistently too high because any amount of oil flushing will lead to the condition where S_{XO} is greater than or equal to S_{WD}.

It appears that the most accurate log-based S_W interpretation method is the Waxman-Smits. It also appears that during the drilling of most wells in the South Pierson Field, very little flushing of oil occurs around the wellbore in the Lower Amaranth Formation. This lack of oil mobility can be attributed to the low permeability in the Lower Amaranth and may be compounded by clay swelling.

Figure 8 shows how the modified Archie S_W values (Equation 15) correlate with S_{WW}. This correlation should be used to correct the modified Archie S_W from Equation (15) to match the Waxman-Smits S_W. This is called the quick-look water saturation S_{WMA} (see also Appendix D).

LOWER AMARANTH POOL DESCRIPTIONS

The Lower Amaranth Formation in all the wells in the study area has been analysed for Lower Amaranth clay content, total and effective porosities, water saturation and original oil-in-place per unit area. Appendix D lists the results. Primary recovery estimates were made for the A and B Pools. The remaining three Lower Amaranth pools are poorly defined. A lack of production history from all pools makes it difficult to accurately estimate recoverable reserves. General history and reserves information for all five South Pierson Lower Amaranth pools are listed in Table 1.

The average total porosity and water saturation for the pools are summarized here:

Pool	Total Porosity	Water Saturation
A	10%	37%
B	12%	32%
C	16%	23%
D	14%	37%
E	9%	49%

Figure 9 is an oil-in-place per unit area map for the Lower Amaranth Formation.

The estimated oil-in-place for the A Pool is 1 361 626 m^3. The wells 9-24-2-29 WPM, 12-19-2-28 WPM and 2-30-2-28 WPM are roughly in the centre of the pool. The reservoir becomes tight to the north and structurally lower and wet to the south of these wells.

The estimated oil-in-place for the B pool is 5 466 428 m^3. There appear to be three oil "pods" in the pool. The first is centered around the well 8-8-2-29 WPM, the second around the well 6-10-2-29 WPM and a third may be centered at 8-16-2-29 WPM. The reservoir dips to the south and becomes tight and wet. The well 6-4-2-29 WPM which is officially part of the B Pool has been mapped separately from the B Pool due to the lack of well control at the south end of the pool.

The remaining three small and isolated pools have not been mapped.

PRODUCTION DECLINE AND RECOVERY FACTORS

The assumed economic limit for oil production in the Lower Amaranth in the South Pierson Field is 0.5 m^3 per day per well. Because of low productivity and modest production decline rates the determination of recoverable reserves by decline analysis is relatively insensitive to the economic limit.

A) South Pierson Lower Amaranth A Pool

The A pool has been developed continuously since its discovery and an average pool production decline cannot be obtained. The only well which shows a consistent production decline rate is the well 9-24-2-29 WPM. The exponential production decline rate for this well is estimated to be 8.1% per year (see Figure 10).

Assuming no further pool development and a current total production of 113 m^3 per month (August 1989), the remaining recoverable reserves for the developed spacing units in the pool are 9 804 m^3 oil. The total oil recovered to August 31, 1989 is 8 918 m^3, giving a primary recovery of 18 722 m^3 or 24% of the original oil-in-place underlying the developed spacing units. Assuming no further development occurs in the pool, the primary recovery will only be 1.4% of the original oil-in-place in the pool.

If the pool is fully developed on 16 hectare spacing, the estimated potential recoverable reserves are 326 790 m^3 oil or 24% of the original oil-in-place and the potential remaining recoverable reserves are 317 872 m^3.

B) South Pierson Lower Amaranth B Pool

A total pool production decline estimate is not possible because of active development throughout the pool's production history. Four wells in the pool show consistent declines.

Well	Decline Rate
16-5-2-29 WPM	25%
16-8-2-29 WPM	9%
14-9-2-29 WPM	15%
4-15-2-29 WPM	12%

The average exponential production decline for the four wells is 12% per year. Figure 11 shows the combined production history decline for the four wells.

Assuming no further pool development and a current total production of 1 860 m^3 per month (August 1989), the remaining recoverable reserves for the developed spacing units in the pool are 160 176 m^3 oil. The total oil recovered to August 31, 1989 is 43 675 m^3, giving a primary recovery of 203 851 m^3 or 16% of the original oil-in-place underlying the developed spacing units. Assuming no further development occurs in the pool, the primary recovery will be 3.7% of the original oil-in-place.

If the pool is fully developed on 32 hectare spacing, the estimated potential recoverable reserves are 874 628 m^3 oil or 16% of the original oil-in-place and the potential remaining reserves are 830 953 m^3.

OIL PRODUCTION AND OIL-IN-PLACE

Figure 12 is an oil-in-place versus production correlation for the Lower Amaranth Formation in the study area. The points marked as "x" are used to obtain an excellent straight line correlation between original oil-in-place and average production. With the exception of a few wells, oil production is correlatable to oil-in-place. There are a few wells which obviously do not fit the correlation. These are summarized below:

A)Underachievers

6-4-2-29 WPM:

This well is structurally low and produced at high water cuts before being converted to a salt water disposal well.

6-10-2-29 WPM:

No reason can be found to explain this well's apparent underachievement.

6-19-2-29 WPM:

This C Pool well produces 4 m^3 oil per day with a low WOR but does not appear to be producing to its full potential. This is the only Lower Amaranth producer in South Pierson which has not been stimulated. A stimulation treatment might result in a higher oil production rate. A stimulation treatment may also result in increased water production.

B)Overachievers

12-30-2-28 WPM:

Production allocation for this well is suspect. This well was reported as the South Pierson Lower Amaranth A Pool discovery well. The completion history for 12-30-2-28 WPM is outlined here:

- July 17/81-perforated and acidized in the Mississippian (993.5 - 998 m)
- July 24/81-bridge plug set at 990 m; Lower Amaranth completed (979 - 986 m)
- July 28/81-Lower Amaranth fraced
- Sept. 5/81-well put on production in Lower Amaranth
- June 1/82-well recompleted to Mississippian

Figure 13 shows the production history for 12-30-2-28 WPM. From September 1981 to May 1982, official records show production from the Lower Amaranth. The well was recompleted to the Mississippian and production resumed in June 1982. Mississippian production trends from June 1982 onward appear to match those from the first nine months of Lower Amaranth production. A large fracture treatment was performed on the Lower Amaranth on completion. The underlying Mississippian cap rock is thin (less than 2 metres). In all probability, the stimulation created some communication between the two zones. The well's first nine months of production may partially or wholly be Mississippian production.

14-4-2-29 WPM:

This well appears to be located at the extreme southern edge of the B Pool. An active aquifer may be supporting production at this well location. Production statistics for this well show an annual production decline of 44%. At this rate of decline, production will quickly decrease to predictably lower levels.

16-5-2-29 WPM:

This well also appears to be located at the extreme southwestern edge of the B Pool. It's production may also be supported by an active aquifer. The annual production decline is 25%. Production is expected to quickly decline to lower levels.

16-9-2-29 WPM:

No reason can be found to explain this well's better-than-expected performance.

FUTURE LOWER AMARANTH POOL DEVELOPMENT

A) Recompletions

Table 2 lists, in order of preference, existing Mississippian producers with Lower Amaranth recompletion potential.

B) Drilling Locations

1) A Pool

There is limited development drilling potential in this pool. If an arbitrary minimum oil-in-place per unit area cutoff of 0.25 m^3/m^2 is used, the following locations show some promise: 10-24-2-28 WPM, 16-24-2-28 WPM, 13-19-2-29 WPM and 3-30-2-29 WPM (see Figure 9). All four locations are offset by producing wells. Assuming a 24% recovery factor on 16 hectare spacing each of these drilling candidates would be expected to recover approximately 9 600 m^3 oil.

2) B Pool

There are a number of locations in the B Pool within the 0.30 m^3/m^2 contour interval (see Figure 9) that are directly offset by producing wells. Assuming a 16% recovery factor and 32 hectare drainage, the minimum recoverable reserves for each well would be 15 360 m^3 oil. Areas that fall within the 0.3 m^3/m^2 contour interval are the east half of Section 8, the west half of Section 9, Section 10, the southwest quarter of Section 15, Section 16 and the east half of Section 17 all in Twp. 2, Rge. 29 WPM. There are 19 undrilled 32 hectare spacing units within these areas.

Table 3 lists, in order of preference, the best Lower Amaranth drilling sites. It should be noted that there appears to be some potential for development in Section 16 and in the east half of Section 17 in Twp. 2, Rge. 29, WPM. Due to the lack of well control in these sections, only the 2-16-2-29 WPM and 6-16-2-29 WPM candidates are included in Table 3.

3) C Pool

The well 6-19-2-29 WPM in the C Pool has the highest original oil-in-place of any of the Lower Amaranth producers in South Pierson. As previously discussed, this well was not fractured, but manages to produce 4 m^3 oil per day.

The C Pool step out well 11-19-2-29 WPM was drilled in August 1989. The only porosity trace run on the well is the Lithodensity tool and consequently accurate porosity and water saturation estimates cannot be made for the well. A Lower Amaranth core was cut from 1 024 to 1 033 metres KB. When the core is analysed, measured porosities will be used to calculate accurate water saturations.

Based on the limited production and log data available the C Pool has some development potential.

CONCLUSIONS

1) The Waxman-Smits equation can be used to calculate accurate water saturations for the Lower Amaranth Formation in the South Pierson Field. Shallow water saturations from the electromagnetic propagation tool match or are slightly higher than Waxman-Smits water saturations. This is a reflection of the very low permeabilities that exist in the Lower Amaranth and indicates that little or no mud filtrate invades the sand.

2) A simple approach can be used to make quick-look calculations of Lower Amaranth porosities and water saturations. The following procedure shows how.

a) from the neutron-density log:

$$\Phi_T = \frac{(0.52\,\Phi_N + \Phi_D)}{1.52}$$

Φ in percentage, sandstone scale

b) from the sonic log:

$\Phi_T = 0.19\Delta t - 37.1$

Φ in percentage

Δt is travel time in µsec/metre

c) if both the sonic and neutron-density logs are available, Φ_T is the average from steps (a) and (b).

d) $S_{WA}{}^2 = \dfrac{0.62 R_W}{\Phi_T{}^{1.59} R_t}$

R_t is the deep resistivity

Φ_T in fractions

if R_w is not known, use 0.04

e) correct S_{WA} using Figure 8 to obtain S_{WMA} where S_{WMA} = Waxman-Smits water saturation

3) The South Pierson Lower Amaranth A Pool appears to have limited recompletion and development drilling potential. One Lower Amaranth recompletion candidate is 10-25-2-29 WPM.

Four development well candidates, in order of preference, are:

1) 10-24-2-29 WPM
2) 13-19-2-28 WPM
3) 16-24-2-29 WPM
4) 3-30-2-29 WPM

4) The South Pierson Lower Amaranth B Pool appears to have substantial recompletion and development drilling potential.

Three B Pool recompletion candidates, in order of preference, are:

1) 8-16-2-29 WPM
2) 8-9-2-29 WPM
3) 14-10-2-29 WPM

Six B Pool development candidates, in order of preference, are:

1) 6-16-2-29 WPM
2) 2-16-2-29 WPM
3) 10-8-2-29 WPM
4) 6-9-2-29 WPM
5) 12-10-2-29 WPM
6) 10-10-2-29 WPM

5) Based on favourable log responses and production records for the well 6-19-2-29 WPM and the initial productivity at 11-19-2-29 WPM, the South Pierson Lower Amaranth C Pool has some development potential.

RECOMMENDATIONS

1) The waterflood potential of the Lower Amaranth in the South Pierson Field should be reviewed. Prior to initiating a waterflood, studies and injectivity tests should be conducted to evaluate clay swelling and fines migration in the Lower Amaranth.

2) Based on the higher recovery factor estimated for the South Pierson Lower Amaranth A Pool the potential of infill drilling on 16 hectare spacing in the South Pierson Lower Amaranth B Pool should be reviewed.

3) The following minimum suite of logs should be run for all South Pierson wells in order to determine important Lower Amaranth reservoir properties:

1) dual induction log
2) compensated neutron-formation density log in tandem or a sonic log or both.

4) More X-Ray diffraction analyses would lead to a better understanding of clay types and percentages in the Lower Amaranth Formation. Such special core analyses may result in better correlations between log responses and clay volume.

5) A thorough evaluation of the Mississippian Mission Canyon Formation and its overlying cap rock might help identify more effective Lower Amaranth completion, stimulation and production methods.

6) The Lower Amaranth and Mission Canyon Formations may have their own unique water analysis profiles. A study of these profiles may help identify Lower Amaranth producers which have been fractured into the Mission Canyon.

REFERENCES

1) Kooyman, R.W., Muir, M.B., Marcinew, R.P., Ben Naceur, K.; 1989: *Effective hydraulic fracturing of the Lower Amaranth Formation in Southern Manitoba.*

2) Core Laboratories, Inc.; 1987: *Petrographic Analysis for Home Oil Company Limited, Home Scurry S. Pierson 8-10-2-29 WPM.*

3) Core Laboratories, Inc.; 1987: *Petrographic Analysis for Home Oil Company Limited, Home et al S. Pierson 6-19-2-29 WPM.*

4) Berry, W.R.; 1983: *Modern Shaly Sand Log Analysis.*

5) Schlumberger Educational Services; 1963: *Schlumberger Log Interpretation Principles/ Applications.*

6) Core Laboratories, Inc.; 1982: *Special Core Analysis.*

7) Pirson, S.J.; 1963: *Handbook of Well Log Analysis For Oil and Gas Formation Evaluation.*

8) Core Laboratories, Inc.; 1982: *Special Core Analysis Study on Omega Waskada Prov. 16-22-1-26 WPM and Omega Waskada 3-25 MC3a-1-26 WPM.*

Appendix A: Nomenclature

a	value of formation factor when Φ_T = 100% on an F vs Φ_T plot
A_c	corrected attenuation (EPT)
A_i	annual production decline (percentage)
AWI	adsorbed water index
B	conductance of the clay exchange cations
1/Boi	oil shrinkage factor
C_{cw}	clay-bound water conductivity
C_t	formation conductivity
C_w	formation water conductivity
CEC	cation exchange capacity
EPT	electromagnetic propagation tool
F	formation factor
F_O	Dual Water Model formation factor
F^*	Waxman-Smits formation factor
GR	log gamma ray reading
K_{ppm}	total dissolved solids in thousands of parts per million (NaCl solution)
m	cementation factor or slope of F vs Φ_T plot
n	saturation exponent
OOIP	original oil-in-place
Q_v	cation concentration per unit volume of fluid in pore space
R_{mf}	resistivity of mud filtrate
$R_{mf\ EPT}$	Rmf calculated from EPT CRIM
R_O	wet formation resistivity
R_t	formation (deep) resistivity
R_W	formation water resistivity
RR	remaining reserves
S_{WA}	Archie water saturation
S_{Wb}	bound water saturation
S_{WD}	Dual Water Model water saturation
S_{WEPT}	Electromagnetic Propagation water saturation
S_{WMA}	modified Archie water saturation
S_{WW}	Waxman-Smits water saturation
S_{XO}	water saturation in flushed zone
t_{pl}	propagation time (EPT)
V_{CLAY}	clay volume
V_{qh}	volume of bound water per unit mass of cations
WOR	water to oil ratio
XRD	X-ray diffraction
β	equivalent conductivity of sodium cations in the Dual Water Model
ρb_{log}	log bulk density
ρ_{ma}	matrix density
ϵ'	dielectric permittivity constant (EPT)
ϵ''	dielectric permittivity constant (EPT)
ϵ'_m	matrix dielectric permittivity constant (EPT)
ϵ'_w	dielectric permittivity constant of water (EPT)
δ	loss tangent (EPT)
δ_w	loss tangent of water (EPT)
Φ_D	log density porosity-sandstone scale
Φ_e	effective porosity
Φ_{EPT}	water-filled porosity (electromagnetic propagation tool)
Φ_N	log neutron porosity-sandstone scale
Φ_S	sonic porosity
Φ_T	total porosity
Φ_{Wb}	bound water porosity
Δt	sonic travel time
Δt_{fl}	fluid travel time
Δt_{ma}	matrix travel time

Appendix B: South Pierson Formation Water Resistivities

Location	Rw
14-5-2-28	0.061
15-5-2-28	0.057
A15-5-2-28	0.057
1-9-2-28	0.055
1-11-2-28	0.055
12-19-2-28	0.042
12-27-2-28	0.044
15-27-2-28	0.046
10-28-2-28	0.042
16-29-2-28	0.046
2-30-2-28	0.042
5-30-2-28	0.042
11-30-2-28	0.043
12-30-2-28	0.046
4-34-2-28	0.043
6-34-2-28	0.046
7-34-2-28	0.045
4-1-2-29	0.042
6-4-2-29	0.040
14-4-2-29	0.038
16-5-2-29	0.042
6-7-2-29	0.042
8-8-2-29	0.043
11-8-2-29	0.040
16-8-2-29	0.041
4-9-2-29	0.038
8-9-2-29	0.039
12-9-2-29	0.039
14-9-2-29	0.039
16-9-2-29	0.039
6-10-2-29	0.038
8-10-2-29	0.040
14-10-2-29	0.040
16-10-2-29	0.044
16-11-2-29	0.044
4-15-2-29	0.044
10-15-2-29	0.040
8-16-2-29	0.039
6-17-2-29	0.038
6-19-2-29	0.044
4-21-2-29	0.044
10-21-2-29	0.044
3-24-2-29	0.041
9-24-2-29	0.043
14-24-2-29	0.043
7-25-2-29	0.044
8-25-2-29	0.042
9-25-2-29	0.042
10-25-2-29	0.044
11-25-2-29	0.042
16-25-2-29	0.044
12-26-2-29	0.043
6-28-2-29	0.044
13-32-2-29	0.048
15-32-2-29	0.036
12-33-2-29	0.045
14-33-2-29	0.044

Appendix C: Electromagnetic Propagation "CRIM"

The following steps describe the iteration method[5] required to solve for S_{XO}. Refer to Appendix A for nomenclature.

1) use R_{mf} from log header information to estimate K_{ppm}

2) solve for ε':

$$\varepsilon' = 0.09 t_{pl}^{\,2} - 2.4972 \times 10^{-5} A_c^{\,2}$$

3) solve for ε'':

$$\varepsilon'' = 1.832 \times 10^{-4} A_c\, t_{pl}$$

4) solve for δ :

$$\tan\delta = \frac{\varepsilon''}{\varepsilon'}$$

5) solve for ε'_w:

$$\varepsilon'_w = 94.88 - .2317T + .000217T^{\,2} - .1556 - .413(K_{ppm}) + .00158(K_{ppm})^2 \quad (T \text{ in degrees F})$$

6) solve for δ_w:

$$\varepsilon'_w \tan\delta_w = 5.66 + 2.65(K_{ppm}) - .0045(K_{ppm})^2$$

7) solve for Φ_{EPT}:

$$\frac{(\varepsilon')^{1/2}}{(1-\tan^2\delta_{w/2})^{1/2}} = \frac{\Phi_{EPT}\,(\varepsilon'_w)^{1/2}}{1-\tan^2\delta_{w/2})^{1/2}} + (1-\Phi_{EPT})(\varepsilon'_m)^{1/2}$$

$\varepsilon'_m = 4.65$ for sandstones

8) solve for δ_W:

$$\frac{(\varepsilon'_w \tan\delta_{/2})^{1/2}}{(1-\tan^2\delta_{/2})^{1/2}} = \frac{\Phi_{EPT}\,(\varepsilon'_w \tan\delta_{/2})^{1/2}}{(1-\tan^2\delta_{w/2})^{1/2}}$$

9) use δ_W from (8) to solve for new K_{ppm} with (6)

10) use K_{ppm} from (9) to solve for new ε'_w with (5)

11) solve for new Φ_{EPT} with (7) and solve for new δ_w with (8)

12) repeat steps (9) through (11) until iteration is no longer required; at this point, Φ_{EPT} is known and the true R_{mf} can be calculated, knowing K_{ppm}

13) solve for S_{XO}:

$$S_{X0} = \frac{\Phi_{EPT}}{\Phi_T}$$

Appendix D: South Pierson Lower Amaranth Petrophysical Calculations

location	top depth (m)	bottom depth (m)	Vclay CFND (%)	Vclay GR (%)	Vclay ave. (%)	CNFD total porosity (%)	CNFD effective porosity (%)	sonic total porosity (%)	average total porosity (%)	Sw Waxman Smits	Sw Dual Water	SwMod Archie a =. 62 m=1.59	OOIP per m ^{2} area
14-5-2-28	992.6	993.7	10	15	12	5.1	2.1	8.5	6.8	0.65	0.88	0.74	.022
DUAL IND	995.5	996.6	39	15	27	6.7	2.7	6.6	6.6	0.43	0.28	0.59	0.035
	996.6	999.0	2	10	6	9.6	7.4	7.0	8.3	0.41	0.57	0.51	0.098
	1000.0	1001.0	18	20	19	8.8	5.3	10.0	9.4	0.45	0.67	0.57	0.044
	1003.5	1005.4	6	10	8	0.1	0.0	2.4	1.3	1.00		1.00	0.000
15-5-2-28	3242.0	3248.0		10	10			12.3	12.3	0.35		0.44	0.122
IE	3254.0	3262.0		10	10			5.6	5.6	0.38		0.51	0.072
	3268.0	3272.0		6	6			7.5	7.5	0.51		0.59	0.038
	3277.0	3284.0		18	18			9.5	9.5	0.39		0.52	0.104
1-9-2-28	980.0	981.0		20	20			8.9	8.9	0.51		0.63	0.036
DUAL IND	983.0	984.0		13	13			5.3	5.3	0.86		0.90	0.006
	985.0	987.5		13	13			6.0	6.0	0.50		0.63	0.063
	988.5	990.0		12	12			4.3	4.3	0.88		0.92	0.007
	994.0	995.5		8	8			2.8	2.8	1.00		1.00	0.000
1-11-2-28	3143.0	3146.0		25	25			11.4	11.4	0.43		0.56	0.050
IE	3151.0	3154.0		24	24			11.4	11.4	0.43		0.56	0.050
	3159.0	3165.0		18	18			8.9	8.9	0.30		0.45	0.095
	3170.0	3174.0		22	22			6.6	6.6	0.55		0.68	0.031
	3188.0	3197.0		12	12			6.6	6.6	0.61		0.70	0.060
12-19-2-28	978.0	978.8		19	19			12.3	12.3				
DUAL IND	9.4	980.3		20	20			10.4	10.4				
	982.0	983.0		17	17			7.9	7.9				
	985.0	986.7		18	18			5.6	5.6				
12-27-2-28	957.8	959.0	46	22	34	7.8	3.8	7.9	7.9	0.60	0.34	0.72	0.031
DUAL IND	960.5	961.4	15	21	18	9.1	5.8	7.0	8.1	0.54	0.66	0.64	0.028
	963.0	965.0	10	18	14	8.1	5.1	6.6	7.4	0.37	0.56	0.50	0.079
	966.0	967.5	10	15	12	3.1	0.1	0.5	1.8	1.00		1.00	0.000
15-27-2-28	3130.0	3132.5		11	11			6.6	6.6	0.80		0.85	0.008
IE	3138.0	3140.0		10	10			6.6	6.6	0.73		0.78	0.009
	3146.0	3152.0		10	10			7.5	7.5	0.40		0.50	0.070
	3158.0	3160.0		2	2			0.9	0.9	1.00		1.00	0.000
	3162.0	3164.0		11	11			5.6	5.6	0.67		0.74	0.010
10-28-2-28	3161.0	3164.0		17	17			6.6	6.6	0.74		0.81	0.013
IE	3170.0	3176.0		11	11			5.6	5.6	0.49		0.60	0.045
	3180.0	3182.0		15	15			4.7	4.7	0.77		0.84	0.005
16-29-2-28	3184.0	3186.0		18	18			7.5	7.5	0.69		0.76	0.012
IE	3192.0	3196.0		8	8			3.7	3.7	0.75		0.81	0.010
	3196.0	3198.0		15	15			5.6	5.6	0.46		0.59	0.016
	3204.0	3206.0		17	17			7.5	7.5	0.56		0.66	0.017
2-30-2-28	978.5	979.7	25	23	24	12.2	8.5	10.0	11.1	0.34	0.52	0.47	0.074
DUAL IND	981.0	982.0	10	20	15	11.1	8.1	7.7	9.4	0.43	0.58	0.54	0.045
	984.0	985.8	7	15	11	10.8	7.9	7.5	9.2	0.26	0.43	0.38	0.102
	991.0	992.5	10	18	14	10.1	7.1	7.2	8.7	0.39	0.55	0.51	0.067

Appendix D: South Pierson Lower Amaranth Petrophysical Calculations

location	top depth (m)	bottom depth (m)	Vclay CFND (%)	Vclay GR (%)	Vclay ave. (%)	CNFD total porosity (%)	CNFD effective porosity (%)	sonic total porosity (%)	average total porosity (%)	Sw Waxman Smits	Sw Dual Water	SwMod Archie a = .62 m=1.59	OOIP per m^2 area
5-30-2-28	973.2	974.0		10	10			11.2	11.2	0.44		0.51	0.042
DUAL IND	974.8	975.6		15	15			7.0	7.0	0.60		0.69	0.019
	977.5	978.2		15	15			7.7	7.7	0.53		0.62	0.022
	980.5	982.0		6	6			4.7	4.7	0.61		0.69	0.023
11-30-2-28	975.0	976.0		24	24			7.0	7.0	0.64		0.73	0.021
DUAL IND	978.0	978.6		19	19			6.2	6.2	0.65		0.74	0.011
	980.0	982.0		15	15			6.2	6.2	0.43		0.55	0.060
	984.3	985.4		28	28			4.7	4.7	0.89		0.93	0.005
	987.0	988.0		21	21			5.8	5.8	0.68		0.77	0.016
12-30-2-28	975.0	976.0		18	18			10.4	10.4				
LATEROLOG	978.0	979.0		15	15			8.5	8.5				
	980.0	980.6		12	12			12.3	12.3				
	980.6	981.0		0	0			13.6	13.6				
	981.0	981.7		12	12			8.9	8.9				
	981.7	982.2		0	0			14.2	14.2				
	982.2	983.2		10	10			7.0	7.0				
	985.0	987.0		0	0			0.0	0.0				
4-34-2-28	3130.0	3134.0		22	22			6.6	6.6	0.85		0.89	0.010
DUAL IND	3136.0	3140.0		27	27			7.5	7.5	0.67		0.76	0.025
	3146.0	3154.0		15	15			3.7	3.7	0.66		0.76	0.026
	3158.0	3163.0		18	18			3.7	3.7	0.86		0.90	0.007
6-34-2-28	951.0	952.0	29	20	24	9.8	6.1		9.8	0.59	0.75	0.67	0.034
DUAL IND	956.2	958.0	7	18	12	8.8	5.9		8.8	0.33	0.54	0.44	0.089
	959.8	960.4	39	16	27	6.7	2.7		6.7	0.51	0.55	0.64	0.016
	963.0	964.0	62	20	41	5.7	1.4		5.7	0.61		0.74	0.018
7-34-2-28	947.0	948.0		16	16			9.5	9.5	0.54		0.63	0.036
DUAL IND	948.7	949.8		15	15			6.6	6.6	0.79		0.83	0.013
	951.0	951.8		20	20			7.5	7.5	0.67		0.75	0.017
	954.0	955.6		11	11			5.8	5.8	0.53		0.62	0.037
	957.2	958.5		3	3			0.0	0.0				
	960.7	961.6		20	20			3.9	3.9	0.96		0.97	0.001
4-1-2-29	1013.0	1014.0	8	6	7	8.0	5.0	6.6	7.3	0.64	0.81	0.70	0.022
DUAL IND	1016.4	1018.7	4	0	2	5.3	2.7	4.7	5.0	0.69	0.90	0.75	0.029
	1019.2	1020.0	10	12	11	9.1	6.1	7.5	8.3	0.49	0.67	0.58	0.029
	1021.8	1022.9	2	12	7	22.1	20.2	21.2	21.7	0.28	0.36	0.33	0.144
	1022.9	1024.4	4	10	7	10.1	7.7	6.6	8.4	0.50	0.62	0.58	0.052
	1028.8	1031.0	8	2	5	3.5	0.5	2.4	2.9	1.00	1.00	1.00	0.000
6-4-2-29	1024.5	1025.4	7	21	14	13.8	10.9		13.8	0.35	0.52	0.44	0.068
PHASOR IND	1025.8	1026.7	5	16	11	11.4	8.8		11.4	0.36	0.54	0.45	0.056
	1029.0	1030.0	2	11	7	11.1	8.9		11.1	0.36	0.52	0.44	0.060
	1033.0	1034.0	4	10	7	10.1	7.7		10.1	0.40	0.58	0.49	0.051
	1034.0	1034.3	4	12	8	14.8	12.2		14.8				
	1034.3	1035.5	2	4	3	9.1	7.2		9.1	0.46	0.61	0.53	0.049

Appendix D: South Pierson Lower Amaranth Petrophysical Calculations

location	top depth (m)	bottom depth (m)	Vclay CFND (%)	Vclay GR (%)	Vclay ave. (%)	CNFD total porosity (%)	CNFD effective porosity (%)	sonic total porosity (%)	average total porosity (%)	Sw Waxman Smits	Sw Dual Water	SwMod Archie a = .62 m=1.59	OOIP per m^2 area
	1037.0	1038.0	10	19	14	14.1	11.1		14.1	0.34	0.51	0.43	0.078
	1040.0	1042.0	3	0	1	3.3	1.0		3.3	1.00	1.00	1.00	0.000
14-4-2-29	1023.0	1023.8	10	15	12	8.1	5.1		8.1	0.46	0.68	0.65	0.030
PHASOR IND	1026.0	1027.0	6	5	6	6.1	3.4		6.1	0.54	0.78	0.73	0.023
	1028.0	1029.4	18	15	16	12.8	9.3		12.8	0.20	0.41	0.40	0.120
	1029.4	1030.0	25	10	17	6.2	2.5		6.2	0.39	0.64	0.58	0.019
	1030.0	1032.0	6	0	3	3.1	0.4		3.1	0.60	0.90	0.78	0.021
16-5-2-29	1023.5	1024.2	10	25	17	10.1	7.1	7.6	8.8	0.37	0.55	0.56	0.033
DUAL IND	1026.8	1027.7	4	18	11	8.3	5.7	5.1	6.7	0.45	0.60	0.64	0.028
	1029.0	1030.0	4	24	14	13.1	10.7	11.5	12.3	0.24	0.4	0.44	0.079
	1030.0	1030.3	8	27	18	17.0	14.0	15.2	16.1				
	1030.3	1031.3	5	15	10	8.4	5.8	2.2	5.3	0.46	0.55	0.65	0.024
	1031.3	1031.7	8	24	16	15.5	12.5	10.4	12.9				
	1031.7	1033.0	2	15	8	6.1	4.2	1	3.7	0.60	0.53	0.78	0.016
6-7-2-29	1030.5	1031.5	4	15	10	8.3	5.7	6.2	7.2	0.56	0.72	0.75	0.027
DUAL IND	1034.0	1035.0	2	0	1	1.3	0.0	0.9	1.1	1.00		1.00	0.000
	1037.3	1040.0	5	11	8	9.4	6.8	7.5	8.5	0.42	0.59	0.60	0.113
	1042.5	1043.8	11	18	15	10.8	7.6	7.0	8.9	0.52	0.67	0.71	0.046
	1045.0	1046.2	4	2	3	1.1	0.0	2.2	1.7	1.00		1.00	0.000
8-8-2-29	1026.0	1027.0	25	21	23	15.2	11.5		15.2	0.26	0.45	0.45	0.094
PHASOR IND	1027.5	1028.4	10	13	11	11.1	8.1		11.1	0.32	0.51	0.51	0.057
	1030.0	1032.0	2	8	5	12.6	10.4		12.6	0.23	0.37	0.43	0.162
	1032.0	1032.3	5	15	10	19.4	16.8		19.4				
	1032.3	1033.7	2	6	4	11.1	8.9		11.1	0.23	0.38	0.43	0.100
	1035.3	1036.0	21	20	21	13.5	9.9		13.5	0.29	0.49	0.49	0.056
11-8-2-29	1025.0	1026.5		22	22			7.4	7.4	0.35		0.54	0.060
DUAL IND	1029.0	1030.0		21	21			10.4	10.4	0.31		0.51	0.060
	1032.6	1035.0		21	21			7.7	7.7	0.30		0.49	0.109
	1039.0	1041.0		17	17			6.6	6.6	0.49		0.68	0.057
16-8-2-29	1019.2	1020.0	2	15	8	12.6	10.4	8.5	10.5	0.33	0.45	0.53	0.047
DUAL IND	1022.0	1022.6	2	10	6	11.4	9.4	5.6	8.5	0.48	0.59	0.67	0.022
	1025.0	1026.5	3	14	8	12.8	10.5	12.3	12.5	0.22	0.37	0.42	0.122
	1026.5	1027.0	4	21	12	16.1	13.7	18.4	17.2				
	1027.0	1027.5	5	11	8	10.4	7.8	5.1	7.8	0.35	0.48	0.54	0.021
	1027.5	1029.0	0	11	6	14.7	13.7	2.4	8.6	0.33	0.44	0.52	0.073
	1032.0	1032.6	3	15	9	13.8	11.5	10.4	12.1	0.34	0.46	0.54	0.040
	1034.0	1035.0	5	7	6	5.4	2.8	4.1	4.8	0.86	0.99	1.00	0.006
4-9-2-29	1021.0	1022.0	3	16	10	11.9	9.6		11.9	0.32	0.49	0.52	0.068
PHASOR IND	1024.0	1025.0	11	15	13	9.3	6.1		9.3	0.40	0.62	0.59	0.047
	1026.6	1027.6	6	15	10	13.6	10.9		13.6	0.24	0.41	0.44	0.086
	1027.0	1027.6	10	22	16	17.1	14.1		17.1				
	1027.6	1028.6	1	10	6	13.4	11.7		13.4	0.21	0.33	0.41	0.089
	1028.6	1029.0	5	16	11	16.4	13.8		16.4				

Appendix D: South Pierson Lower Amaranth Petrophysical Calculations

location	top depth (m)	bottom depth (m)	Vclay CFND (%)	Vclay GR (%)	Vclay ave. (%)	CNFD total porosity (%)	CNFD effective porosity (%)	sonic total porosity (%)	average total porosity (%)	Sw Waxman Smits	Sw Dual Water	SwMod Archie a=.62 m=1.59	OOIP per m^2 area
	1029.0	1030.4	4	5	4	4.6	2.2		4.6	0.44	0.71	0.63	0.030
	1034.6	1035.6	3	11	7	8.8	6.5		8.8	0.44	0.63	0.63	0.041
8-9-2-29	1016.6	1017.6	6	15	10	12.1	9.4		12.1	0.36	0.53	0.44	0.066
PHASOR IND	1019.4	1020.6	8	15	11	10.0	7.0		10.0	0.38	0.59	0.49	0.062
	1022.0	1023.2	3	5	4	11.4	9.1		11.4	0.25	0.40	0.33	0.086
	1023.2	1023.8	6	15	10	16.6	13.9		16.6				
	1023.8	1025.0	3	5	4	6.8	4.5		6.8	0.34	0.55	0.44	0.045
12-9-2-29	1016.7	1017.9	18	21	19	11.8	8.3	11.4	11.6	0.31	0.52	0.43	0.080
PHASOR IND	1020.6	1021.4	7	15	11	12.3	9.4	10.4	11.3	0.34	0.51	0.44	0.050
	1023.0	1024.8	3	10	6	12.8	10.5	9.8	11.3	0.24	0.37	0.31	0.130
	1024.8	1025.3	5	15	10	18.4	15.8	14.2	16.3				
	1025.3	1026.4	2	2	2	6.6	4.4	3.6	5.1	0.42	0.58	0.52	0.027
	1028.3	1029.1	33	21	27	11.5	7.6	10.4	11.0	0.32	0.54	0.46	0.050
	1030.0	1032.0	10	15	12	11.1	8.1	8.5	9.8	0.38	0.56	0.49	0.102
14-9-2-29	1017.5	1018.0	13	21	17	13.5	10.2	10.4	11.9	0.34	0.51	0.45	0.033
PHASOR IND	1020.4	1021.0	6	19	13	13.6	10.9	8.7	11.2	0.39	0.52	0.49	0.034
	1023.7	1024.7	2	11	7	14.1	11.9	6.2	10.2	0.30	0.41	0.39	0.060
	1025.0	1026.0	2	5	3	9.1	7.2	2.8	5.9	0.39	0.51	0.49	0.031
	1030.0	1031.5	10	15	12	12.6	9.6	10.0	11.3	0.41	0.56	0.50	0.085
	1032.0	1033.0	15	10	13	10.1	6.8	7.5	8.8	0.53	0.70	0.62	0.035
16-9-2-29	1012.2	1013.0	18	22	20	12.8	9.3	12.3	12.6	0.36	0.56	0.47	0.054
PHASOR IND	1014.0	1015.0	6	18	12	12.1	9.4	10.4	11.3	0.39	0.55	0.48	0.058
	1015.3	1016.0	15	24	20	13.1	9.8	12.5	12.8				
	1016.6	1017.0	7	24	16	11.8	8.9	11.4	11.6	0.40	0.58	0.50	0.023
	1019.5	1020.3	2	13	7	13.1	11.2	7.0	10.0	0.29	0.41	0.39	0.048
	1020.3	1020.6	4	16	10	19.1	16.7	14.6	16.8				
	1020.6	1022.0	6	2	4	2.1	0.0	1.3	1.7	1.00		1.00	0.000
	1024.0	1025.0	15	21	18	13.1	9.8	10.4	11.8	0.34	0.52	0.45	0.065
	1026.2	1027.3	25	10	17	8.2	4.5	6.6	7.4	0.61	0.78	0.70	0.027
	1028.0	1028.6	7	10	9	7.8	4.9	6.6	7.2	0.64	0.82	0.71	0.013
6-10-2-29	1014.0	1014.7	2	24	13	11.4	9.4	12.3	11.9	0.31	0.50	0.42	0.048
PHASOR IND	1015.0	1016.0		33	33			11.4	11.4	0.29		0.43	0.068
	1018.0	1018.8	2	18	10	10.4	8.4	11.4	10.9	0.35	0.53	0.44	0.048
	1020.5	1021.4	2	11	6	12.1	10.2	11.4	11.7	0.21	0.35	0.30	0.070
	1021.4	1021.8	4	15	10	17.3	14.7	13.4	15.4	0.16	0.26	0.24	0.043
	1021.8	1023.0	2	5	3	8.1	6.2	8.5	8.3	0.18	0.36	0.28	0.069
	1023.0	1023.5		5	5			19.9	19.9	0.09		0.14	0.076
	1028.0	1029.0	4	5	4	4.1	1.7	3.2	3.6	0.91	1.00	0.93	0.003
8-10-2-29	1010.5	1011.5	15	23	19	13.1	9.8	11.4	12.2	0.30	0.49	0.42	0.072
PHASOR IND	1012.0	1013.0	13	20	17	12.5	9.2	10.4	11.4	0.30	0.49	0.42	0.067
	1014.6	1015.6	8	16	12	10.0	7.0	7.5	8.8	0.38	0.56	0.49	0.046
	1018.2	1019.2	4	12	8	11.8	9.2	8.3	10.0	0.22	0.36	0.33	0.066
	1019.2	1019.7	10	35	23	17.1	14.1	14.6	15.9				

Appendix D: South Pierson Lower Amaranth Petrophysical Calculations

location	top depth (m)	bottom depth (m)	Vclay CFND (%)	Vclay GR (%)	Vclay ave. (%)	CNFD total porosity (%)	CNFD effective porosity (%)	sonic total porosity (%)	average total porosity (%)	Sw Waxman Smits	Sw Dual Water	SwMod Archie a = .62 m=1.59	OOIP per m^2 area
	1019.7	1021.6	4	5	4	7.1	4.7	3.0	5.0	0.25	0.41	0.38	0.061
	1023.8	1025.0	10	0	5	2.1	0.0	0.3	1.2	1.00		1.00	0.000
	1025.0	1025.4	3	6	5	5.9	3.6	2.8	4.4				
	1025.4	1027.7	4	0	2	0.0	0.0	0.0	0.0				
14-10-2-29	1012.0	1013.0	15	20	18	13.1	9.8		13.1	0.35	0.54	0.45	0.072
PHASOR IND	1013.5	1014.2	8	23	16	12.5	9.5		12.5	0.31	0.50	0.41	0.051
	1016.4	1017.0	10	24	17	12.1	9.1		12.1	0.31	0.51	0.42	0.042
	1019.0	1019.5	6	22	14	13.6	10.9		13.6	0.19	0.36	0.29	0.046
	1019.5	1020.0	7	25	16	17.8	14.9		17.8				
	1020.0	1020.7	2	15	8	13.3	11.3		13.3	0.21	0.35	0.30	0.062
	1020.7	1021.1	7	22	15	17.8	14.9		17.8				
	1021.1	1022.5	4	9	6	4.1	1.7		4.1	0.40	0.66	0.53	0.029
	1024.4	1025.0	21	25	23	10.5	6.9		10.5	0.34	0.57	0.47	0.035
16-10-2-29	1007.0	1008.0	13	20	16	12.5	9.2	12.3	12.4	0.38	0.57	0.48	0.065
DUAL IND	1008.6	1009.4	7	20	14	11.8	8.9	8.5	10.1	0.41	0.56	0.51	0.040
	1010.1	1011.0	25	22	23	13.7	10.0	12.9	13.3	0.36	0.55	0.47	0.064
	1011.6	1012.5	6	11	9	9.1	6.4	6.2	7.7	0.47	0.63	0.57	0.031
	1014.0	1015.7	2	8	5	9.1	7.2	4.7	6.9	0.39	0.51	0.49	0.060
	1016.2	1018.0	3	2	3	3.9	1.6	2.4	3.2	0.45	0.67	0.57	0.027
16-11-2-29	1001.0	1001.7		29	29			12.3	12.3				
LATEROLOG	1002.0	1003.0		27	27			11.9	11.9				
	1003.5	1004.4		24	24			7.7	7.7				
	1006.0	1007.0		27	27			7.5	7.5				
	1009.0	1010.0		12	12			1.7	1.7				
	1010.2	1011.0		20	20			5.3	5.3				
	1013.0	1014.2		23	23			5.6	5.6				
	1015.8	1017.1		16	16			4.7	4.7				
	1017.4	1018.5		15	15			1.3	1.3				
4-15-2-29	1010.0	1011.0	10	32	21	14.1	11.1	11.5	12.8	0.31	0.47	0.42	0.074
DUAL IND	1011.4	1012.2	6	24	15	12.1	9.4	11.0	11.5	0.36	0.53	0.46	0.050
	1014.3	1015.0	6	26	16	13.6	10.9	9.8	11.7	0.35	0.49	0.45	0.045
	1016.5	1018.0	2	16	9	13.1	11.2	8.5	10.8	0.30	0.41	0.40	0.095
	1018.0	1018.8	4	22	13	17.8	15.2	13.8	15.8				
	1018.8	1020.0	4	13	9	5.6	3.2	2.4	4.0	0.61	0.63	0.71	0.016
	1021.4	1022.4	21	28	25	10.5	6.9	9.1	9.8	0.40	0.58	0.52	0.049
10-15-2-29	1004.8	1005.8	10	17	13	11.1	8.1		11.1	0.35	0.55	0.46	0.060
PHASOR IND	1006.5	1007.2	21	23	22	13.5	9.9		13.5	0.34	0.54	0.45	0.053
	1007.7	1008.4	10	23	16	12.6	9.6		12.6	0.37	0.56	0.47	0.047
	1010.5	1011.5	3	11	7	9.8	7.5		9.8	0.28	0.46	0.38	0.059
	1011.5	1012.0	8	18	13	14.5	11.5		14.5				
	1012.0	1012.9	2	5	4	5.1	2.9		5.1	0.48	0.71	0.58	0.020
	1017.0	1018.5	8	11	10	7.0	4.0		7.0	0.57	0.78	0.65	0.038
8-16-2-29	1009.6	1010.2	15	23	19	14.1	10.8		14.1	0.32	0.51	0.42	0.048

Appendix D: South Pierson Lower Amaranth Petrophysical Calculations

location	top depth (m)	bottom depth (m)	Vclay CFND (%)	Vclay GR (%)	Vclay ave. (%)	CNFD total porosity (%)	CNFD effective porosity (%)	sonic total porosity (%)	average total porosity (%)	Sw Waxman Smits	Sw Dual Water	SwMod Archie a =. 62 m=1.59	OOIP per m ^{2} area
PHASOR IND	1010.7	1011.7	13	23	18	14.5	11.2		14.5	0.32	0.50	0.42	0.083
	1012.2	1013.1	18	19	18	12.8	9.3		12.8	0.32	0.53	0.43	0.066
	1015.3	1016.0	8	24	16	14.5	11.5		14.5	0.31	0.49	0.41	0.058
	1018.4	1019.0	2	10	6	11.6	9.4		11.6	0.25	0.41	0.34	0.044
	1019.0	1019.5	5	16	11	18.4	15.8		18.4				
	1019.5	1021.0	2	5	4	8.4	6.4		8.4	0.28	0.46	0.38	0.076
	1022.1	1023.0	13	23	18	13.5	10.2		13.5	0.28	0.47	0.39	0.074
	1025.0	1026.0	15	15	15	10.1	6.8		10.1	0.45	0.67	0.55	0.047
6-17-2-29	1021.0	1022.0	18	16	17	11.8	8.3	11.4	11.6	0.31	0.52	0.42	0.067
PHASOR IND	1024.0	1024.7	15	18	17	11.6	8.3	8.9	10.3	0.41	0.59	0.52	0.036
	1026.8	1027.5	3	9	6	12.8	10.5	9.1	10.9	0.25	0.36	0.34	0.048
	1027.5	1028.0	10	15	12	17.1	14.1	13.4	15.3				
	1028.0	1029.0	4	4	4	4.1	1.7	0.0	2.1	1.00		1.00	0.000
	1034.0	1036.0	0	15	7	19.0	19.0	6.6	12.8	0.30	0.40	0.38	0.150
6-19-2-29	1016.7	1018.0	13	21	17	13.5	10.2		13.5	0.30	0.49	0.41	0.102
DUAL IND	1021.8	1023.4	4	8	6	13.1	10.7		13.1	0.16	0.30	0.24	0.148
	1025.7	1026.6	4	15	9	14.1	11.7		14.1	0.24	0.38	0.32	0.081
	1027.5	1028.4	7	10	8	9.8	6.9		9.8	0.23	0.43	0.33	0.057
	1028.4	1029.0	1	15	8	19.4	18.0		19.4				
	1029.0	1030.6	4	2	3	7.1	4.7		7.1	0.28	0.49	0.37	0.069
	1037.0	1039.0	7	14	11	8.8	5.9		8.8	0.42	0.63	0.52	0.086
4-21-2-29	1012.8	1014.0	8	15	11	9.5	6.5	8.9	9.2	0.46	0.65	0.55	0.050
DUAL IND	1014.4	1015.2	29	19	24	11.8	8.1	11.5	11.7	0.41	0.62	0.52	0.046
	1015.9	1016.6	10	15	12	9.1	6.1	8.5	8.8	0.48	0.68	0.58	0.027
	1018.2	1019.5	5	12	9	9.4	6.8	6.8	8.1	0.35	0.52	0.46	0.057
	1019.5	1020.0	8	15	11	15.5	12.5	12.3	13.9				
	1020.0	1020.7	5	12	9	9.4	6.8	7.0	8.2	0.35	0.52	0.45	0.031
	1022.5	1023.4	29	23	26	10.3	6.6	9.3	9.8	0.39	0.59	0.52	0.045
	1025.0	1026.0	10	11	11	8.1	5.1	6.4	7.3	0.66	0.82	0.73	0.021
10-21-2-29	1005.0	1006.3	8	19	14	10.0	7.0		10.0	0.46	0.65	0.55	0.059
PHASOR IND	1008.0	1008.6	13	18	16	10.5	7.2		10.5	0.48	0.68	0.57	0.028
	1010.7	1011.9	2	5	4	8.1	5.9		8.1	0.37	0.55	0.46	0.051
	1011.9	1012.1	6	15	10	12.1	9.4		12.1				
	1012.1	1013.0	4	9	6	6.1	3.7		6.1	0.48	0.70	0.57	0.024
	1014.8	1016.0	13	22	18	9.5	6.2		9.5	0.40	0.62	0.52	0.057
	1017.0	1018.3	4	15	10	5.8	3.2		5.8	0.63	0.81	0.71	0.024
3-24-2-29	994.5	995.2	13	18	16	8.5	5.2		8.5	0.46	0.68	0.57	0.027
DUAL IND	997.0	998.0	7	8	8	8.8	5.9		8.8	0.28	0.50	0.39	0.053
	998.0	998.2	6	15	10	12.1	9.4		12.1	0.20	0.38	0.30	0.016
	998.2	999.0	5	11	8	11.4	8.8		11.4	0.22	0.40	0.32	0.060
	1004.0	1005.0	11	18	15	9.3	6.1		9.3	0.43	0.65	0.54	0.044
9-24-2-29	980.6	981.7		20	20			12.3	12.3	0.33		0.44	0.076
DUAL IND	982.0	983.0		18	18			10.4	10.4	0.37		0.49	0.055

Appendix D: South Pierson Lower Amaranth Petrophysical Calculations

location	top depth (m)	bottom depth (m)	Vclay CFND (%)	Vclay GR (%)	Vclay ave. (%)	CNFD total porosity (%)	CNFD effective porosity (%)	sonic total porosity (%)	average total porosity (%)	Sw Waxman Smits	Sw Dual Water	SwMod Archie a = .62 m=1.59	OOIP per m^2 area
	985.0	986.0		10	10			6.8	6.8	0.46		0.56	0.031
	987.0	988.0		6	6			3.7	3.7	0.50		0.61	0.016
	989.0	989.7		18	18			8.5	8.5	0.23		0.37	0.039
	993.0	994.0		15	15			8.9	8.9	0.48		0.58	0.039
	995.3	996.7		12	12			9.6	9.6	0.40		0.50	0.068
14-24-2-29	983.5	984.2		26	26			8.9	8.9	0.36		0.50	0.034
DUAL IND	984.2	985.5		15	15			1.3	1.3	1.00		1.00	0.000
	990.0	992.0		16	16			3.7	3.7	0.69		0.78	0.020
	993.8	994.8		32	32			9.5	9.5	0.38		0.52	0.049
	996.0	997.0		24	24			8.5	8.5	0.48		0.60	0.037
	997.0	998.0		17	17			6.6	6.6	0.61		0.71	0.021
	998.5	999.8		9	9			0.5	0.5	1.00		1.00	0.000
7-25-2-29	978.0	979.0		23	23			6.6	6.6	0.61		0.71	0.021
DUAL IND	980.5	982.0		24	24			4.7	4.7	0.91		0.94	0.006
	983.0	984.3		11	11			6.2	6.2	0.38		0.50	0.042
	984.3	985.5		11	11			1.8	1.8	1.00		1.00	0.000
	989.3	992.0		0	0			0.0	0.0				
	992.5	993.7		4	4			0.0	0.0				
8-25-2-29	976.0	977.0		24	24			10.0	10.0	0.41		0.54	0.049
DUAL IND	979.0	980.0		15	15			4.7	4.7	0.77		0.83	0.009
9-25-2-29	975.2	976.2		16	16			10.0	10.0	0.45		0.55	0.046
DUAL IND	978.0	979.0		14	14			5.6	5.6	0.72		0.79	0.013
	981.0	982.7		11	11			5.6	5.6	0.49		0.60	0.041
10-25-2-29	977.4	978.4		21	21			11.7	11.7	0.40		0.51	0.059
DUAL IND	979.0	979.7		21	21			10.4	10.4	0.39		0.50	0.037
	981.8	983.0		3	3			0.0	0.0				
	984.5	985.0		13	13			8.7	8.7	0.31		0.42	0.025
	985.4	986.0		16	16			6.6	6.6	0.39		0.52	0.020
	987.7	988.7		20	20			8.5	8.5	0.48		0.59	0.037
	990.0	991.0		15	15			8.5	8.5	0.56		0.64	0.031
	992.0	993.6		10	10			6.0	6.0	0.68		0.74	0.026
11-25-2-29	977.0	978.0		25	25			6.6	6.6	0.60		0.71	0.022
DUAL IND	978.3	979.0		24	24			8.5	8.5	0.45		0.58	0.027
	983.5	984.4		14	14			4.7	4.7	0.53		0.65	0.017
	984.4	984.8		18	18			12.1	12.1				
	984.8	985.7		16	16			4.7	4.7	0.52		0.65	0.017
	991.0	992.0		19	19			7.2	7.2	0.45		0.57	0.033
16-25-2-29	973.5	974.3		33	33			10.4	10.4	0.43		0.56	0.040
DUAL IND	975.0	975.7		26	26			10.4	10.4	0.42		0.54	0.036
	977.5	978.5		27	27			6.6	6.6	0.63		0.73	0.020
	980.5	981.0		24	24			6.6	6.6	0.42		0.56	0.016
	981.0	981.3		27	27			14.8	14.8				
	981.3	982.0		21	21			5.6	5.6	0.51		0.63	0.016

Appendix D: South Pierson Lower Amaranth Petrophysical Calculations

location	top depth (m)	bottom depth (m)	Vclay CFND (%)	Vclay GR (%)	Vclay ave. (%)	CNFD total porosity (%)	CNFD effective porosity (%)	sonic total porosity (%)	average total porosity (%)	Sw Waxman Smits	Sw Dual Water	SwMod Archie a =. 62 m=1.59	OOIP per m ^{2} area
	986.2	987.0		26	26			6.6	6.6	0.70		0.79	0.013
	987.5	988.3		24	24			7.0	7.0	0.66		0.75	0.016
	988.5	989.5		20	20			1.7	1.7	1.00		1.00	0.000
12-26-2-29	986.5	987.2	33	23	28	12.5	8.6	10.8	11.6	0.39	0.58	0.50	0.042
DUAL IND	988.0	989.0	33	23	28	11.5	7.6	10.4	11.0	0.39	0.59	0.51	0.056
	991.0	991.5	11	21	16	12.3	9.1	8.5	10.4	0.46	0.60	0.55	0.024
	993.5	994.5	11	12	12	9.3	6.1	5.6	7.5	0.37	0.54	0.48	0.040
	994.5	995.0	13	16	15	13.5	10.2	12.1	12.8				
	995.0	995.6	10	12	11	8.1	5.1	2.6	5.4	0.52	0.61	0.63	0.013
	997.0	997.8	21	18	19	11.0	7.4	8.5	9.7	0.40	0.59	0.51	0.039
6-28-2-29	1000.7	1001.7		26	26			10.8	10.8	0.42		0.54	0.052
DUAL IND	1002.2	1003.2		26	26			8.5	8.5	0.46		0.58	0.039
	1004.0	1005.0		29	29			12.3	12.3	0.38		0.50	0.064
	1005.0	1006.0		25	25			7.2	7.2	0.67		0.76	0.020
	1008.0	1008.9		21	21			2.8	2.8	1.00		1.00	0.000
	1008.9	1009.2		30	30			9.6	9.6				
	1009.2	1010.0		18	18			1.3	1.3	1.00		1.00	0.000
	1011.6	1012.7		27	27			6.6	6.6	0.59		0.71	0.025
13-32-2-29	3308.0	3310.0		18	18			6.6	6.6	0.82		0.86	0.006
DUAL IND	3318.0	3323.0		10	10			5.6	5.6	0.52		0.62	0.034
	3328.0	3330.0		17	17			4.7	4.7	0.89		0.92	0.003
15-32-2-29	3278.0	3282.0		23	23			12.3	12.3	0.27		0.39	0.093
IE	3306.0	3313.0		18	18			8.5	8.5	0.20		0.34	0.122
12-33-2-29	1004.0	1005.0		15	15			7.0	7.0	0.64		0.72	0.021
DUAL IND	1006.8	1007.5		16	16			7.9	7.9	0.58		0.67	0.019
	1009.9	1010.3		8	8			5.8	5.8	0.56		0.64	0.009
	1010.3	1010.7		10	10			8.7	8.7				
	1010.7	1011.5		9	9			5.6	5.6	0.57		0.66	0.016
	1013.0	1014.0		15	15			6.6	6.6	0.63		0.71	0.020
	1015.4	1016.5		10	10			8.1	8.1	0.54		0.61	0.035
	1017.0	1019.0		5	5			4.7	4.7	0.72		0.77	0.022
14-33-2-29	998.6	999.8		15	15			6.6	6.6	0.77		0.83	0.015
DUAL IND	1001.3	1002.0		20	20			7.0	7.0	0.72		0.79	0.011
	1004.0	1006.0		8	8			2.8	2.8	1.00		1.00	0.000
	1007.6	1009.0		15	15			5.8	5.8	0.68		0.76	0.022
4-36-2-29	976.4	977.0		16	16			6.6	6.6	0.68		0.76	0.011
DUAL IND	977.5	978.6		20	20			7.7	7.7	0.52		0.63	0.034
	983.0	983.7		13	13			6.8	6.8	0.36		0.49	0.026
	983.7	984.0		15	15			10.4	10.4				
	984.0	984.7		12	12			6.0	6.0	0.41		0.54	0.021
	986.3	987.5		18	18			8.5	8.5	0.47		0.58	0.046
	989.6	991.0		10	10			5.1	5.1	0.62		0.71	0.023

Table 1: Reservoir Engineering Properties of the Lower Amaranth Formation

POOL	12 29A	12 29B	12 29C	12 29D	12 29E
General Information					
1. Year of Discovery	1981 (?)	1985	1987	1988	1986
2. Number of wells:					
a) capable of oil production	4	14	1	1	1
b) produced first half of 1989	3	12	1	0	0
c) previous producers	1	1	0	0	0
3. Spacing	16 ha	32 ha	16 ha	16 ha	16 ha
4. Average Depth of Producing Zone	-525 m	-547 m	-543 m	-550 m	-553 m
5. Crude Oil Quality					
a) density	847 kg/m^3	847 kg/m^3	847 kg/m^3	847 kg/m^3	847 kg/m^3
b) sulphur content	0.11%	0.11%	0.11%	0.11%	0.11%
6. Initial Pressure (at datum)	--	10 010 kPa	10 590 kPa	10 730 kPa	--
7. Current Pressure (at datum)	--	9 700 kPa	--	--	--
8. Recovery Mechanism	← low energy natural water drive →				
Reserves Information					
1. Production Area	799 ha	1 751 ha	32 ha	16 ha	16 ha
2. Net Pay	3.2 ha	4.6 m	5.3 m	3.5 m	5.0 m
3. Porosity	10%	12%	16%	14%	9%
4. Connate Water Saturation	37%	32%	23%	37%	49%
5. Shrinkage Factor (1/Boi*)	0.84	0.84	0.84	0.84	0.84
6. Original oil-in-place	1 361 626 m^3	5 466 428 m^3	174 830 m^3	40 470 m^3	30 757 m^3
7. Recovery Factor	1.4%	3.7%	--	--	--
8. Potential Recovery Factor*	24%	16%	--	--	--
9. Recoverable Reserves	18 722 m^3	203 851 m^3	--	--	--
10. Potential Recoverable Reserves*	326 702 m^3	874 628 m^3	--	--	--
11. Cumulative Production (to August 31, 1989)	8 918 m^3	43 675 m^3	2 948 m^3	85 m^3	42 m^3
12. Remaining Recoverable Reserves	9 804 m^3	160 176 m^3	--	--	--
13. Potential Remaining Recoverable Reserves (Aug, 31, 1989)*	154 477 m^3	830 953 m^3	-	-	-

Trap Type for all pools: primarily stratigraphic

* 1/Boi obtained from PVT data

* assuming the A Pool is fully developed on 16 ha spacing and the B Pool is fully developed on 32 ha spacing

Table 2: Lower Amaranth Recompletion Candidates

RECOMPLETION CANDIDATES

Pool	Location	Interval (metres)	Total Porosity (%)	Water Saturation (%)	Ranking (low/medium /high)
B	8-16-2-29 WPM	1 009.5 - 1 023	8.5-18.5	25-32	high
B	8-9-2-29 WPM	1 016.5 - 1 024	10-16.5	25-40	medium-high
B	14-10-2-29 WPM	1 012 - 1 021	12-18	20-35	medium
A	10-25-2-29 WPM	977.5 - 980	7-8.5	30-50	low

OFFSET PRODUCERS

Location(s)	Oil Prod. (m3/d)	WOR (m3/m2)	Annual Production Decline (%)
14-9-2-29	5.7	6.9	15
16-9-2-29	8.6	0.1	--
4-15-2-29	7.2	0.1	12
16-9-2-29	8.6	0.1	--
6-10-2-29	4.7	4.0	--
16-9-2-29	8.6	0.1	--
6-10-2-29	4.7	4.0	--
8-10-2-29	4.0	17.5	
16-10-2-29	produced only water		
4-15-2-29	7.2	0.1	12
12-30-2-2*	Mississippian production suspected		

* Recompleted to the Mississippian - June 1982.

Table 3: Lower Amaranth Drilling Candidates

DRILLING CANDIDATES			*OFFSET PRODUCERS*			
Pool	**Location**	**Ranking (low/medium /high)**	**Location(s)**	**Oil Prod. (m^3/d)**	**WOR m^3/m^3**	**Annual Production Decline (%)**
B	6-16-2-29 WPM	high	8-16-2-29	Lower Amaranth recompletion candidate		
B	2-16-2-29 WPM	high	8-16-2-29	Lower Amaranth recompletion candidate		
B	10-8-2-29 WPM	medium-high	8-8-2-29	10.4	2.1	--
			16-8-2-29	4.8	0.2	9
			12-9-2-29	10.0	0.2	--
B	6-9-2-29 WPM	medium-high	4-9-2-29	5.1	2.8	--
			12-9-2-29	10.0	0.2	--
			14-9-2-29	5.7	6.9	15
B	12-10-2-29 WPM	medium	16-9-2-29	8.6	0.1	--
			6-10-2-29	4.7	4.0	--
B	10-10-2-29 WPM	low-medium	6-10-2-29	4.7	4.0	--
			8-10-2-29	4.0	17.5	--
			16-10-2-29	produced only water		
A	10-24-2-29 WPM	low-medium	8-24-2-29	7.0	0.2	--
			9-24-2-29	2.9	7.1	8
			14-24-2-29	0.7	3.7	--
A	13-19-2-28 WPM	low-medium	12-19-2-28	0.1	0	--
			9-24-2-29	2.9	7.1	8
A	16-24-2-29 WPM	low-medium	9-24-2-29	2.9	7.1	8
			14-24-2-29	0.7	3.7	--

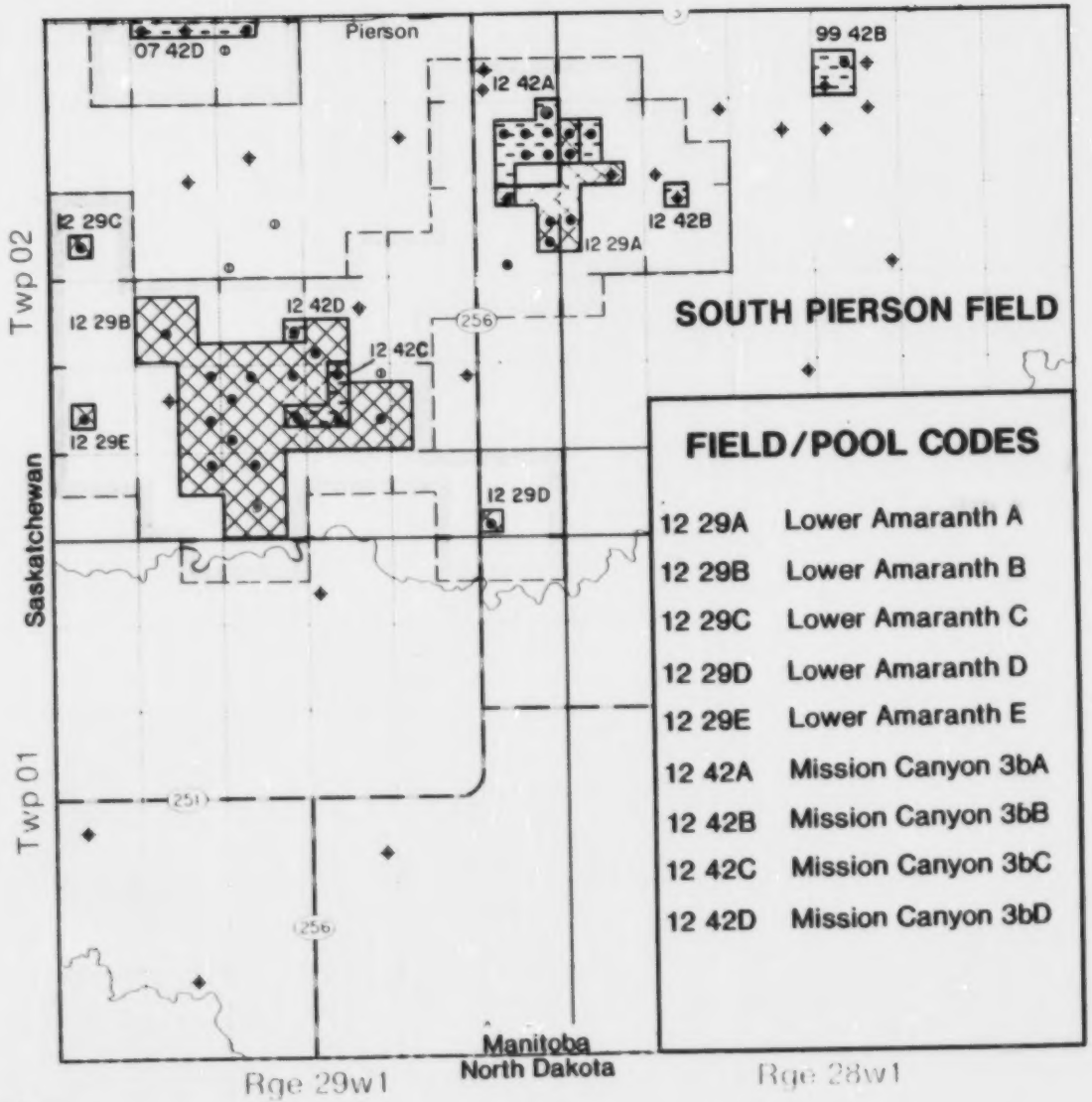

Figure 1: Study Area

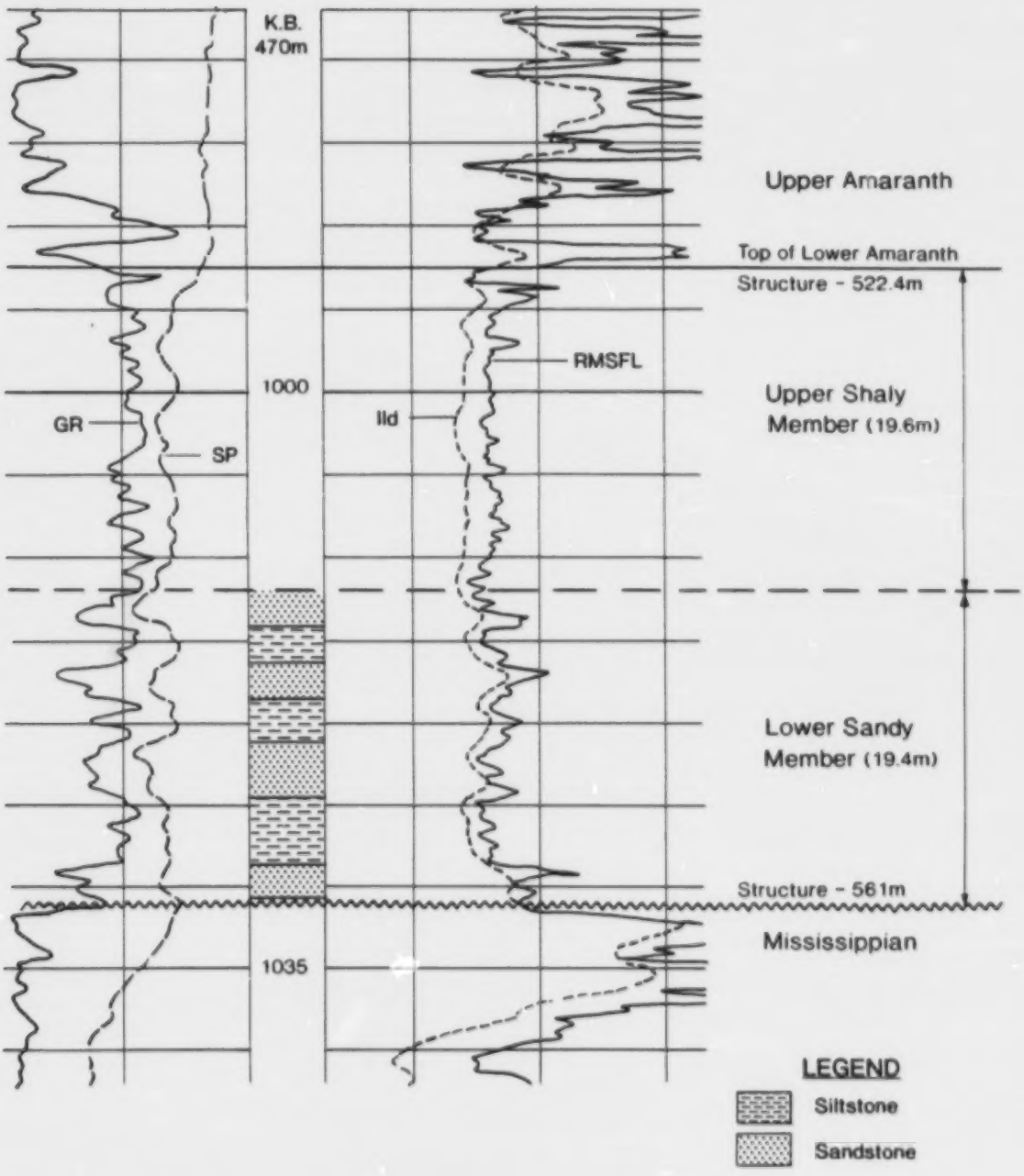

Figure 2: Type Log of Lower Amaranth Formation–Home Scurry S.Pierson 4–1–2–29 WPM

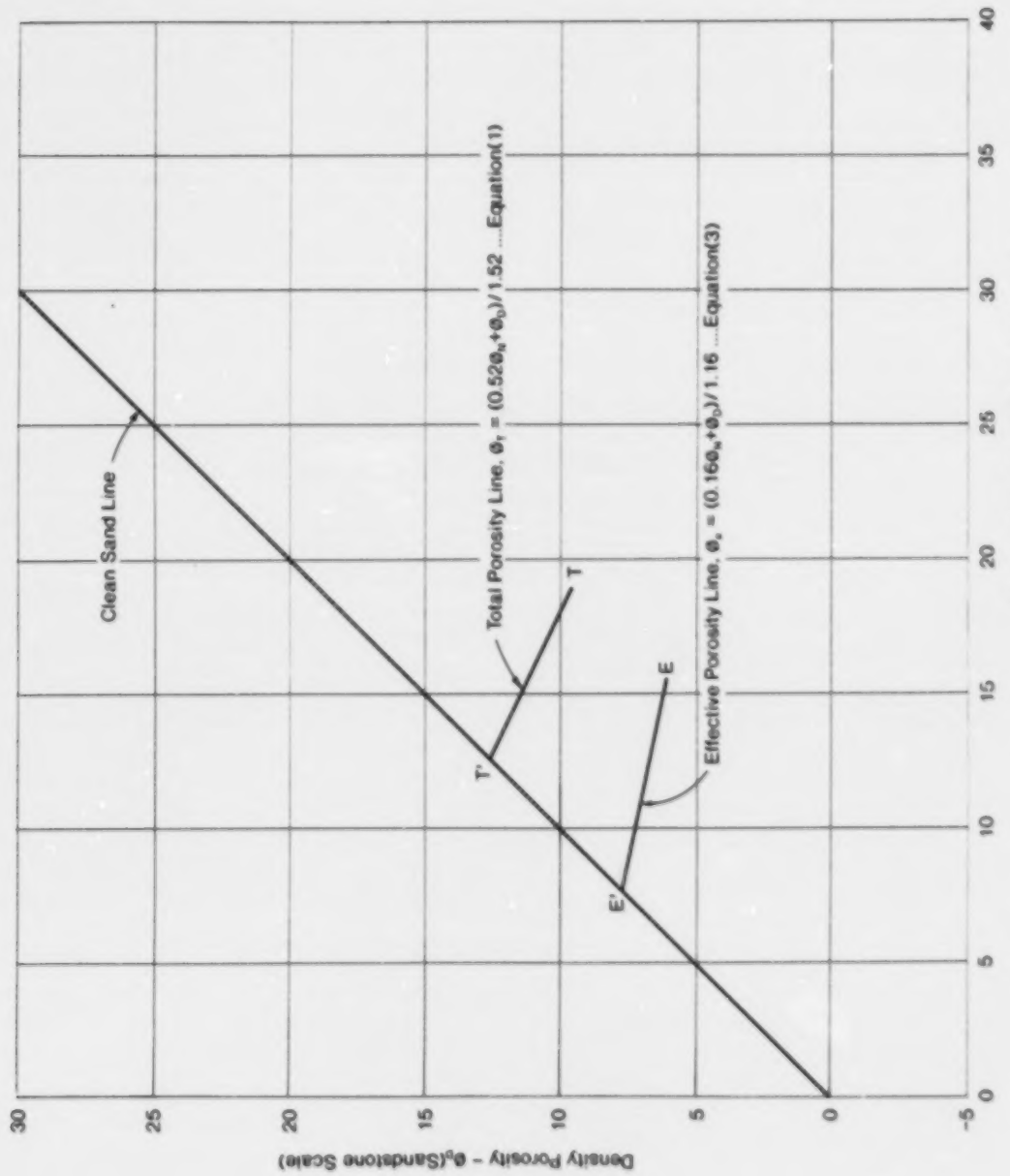

Figure 3: Neutron–Density Porosity Crossplot

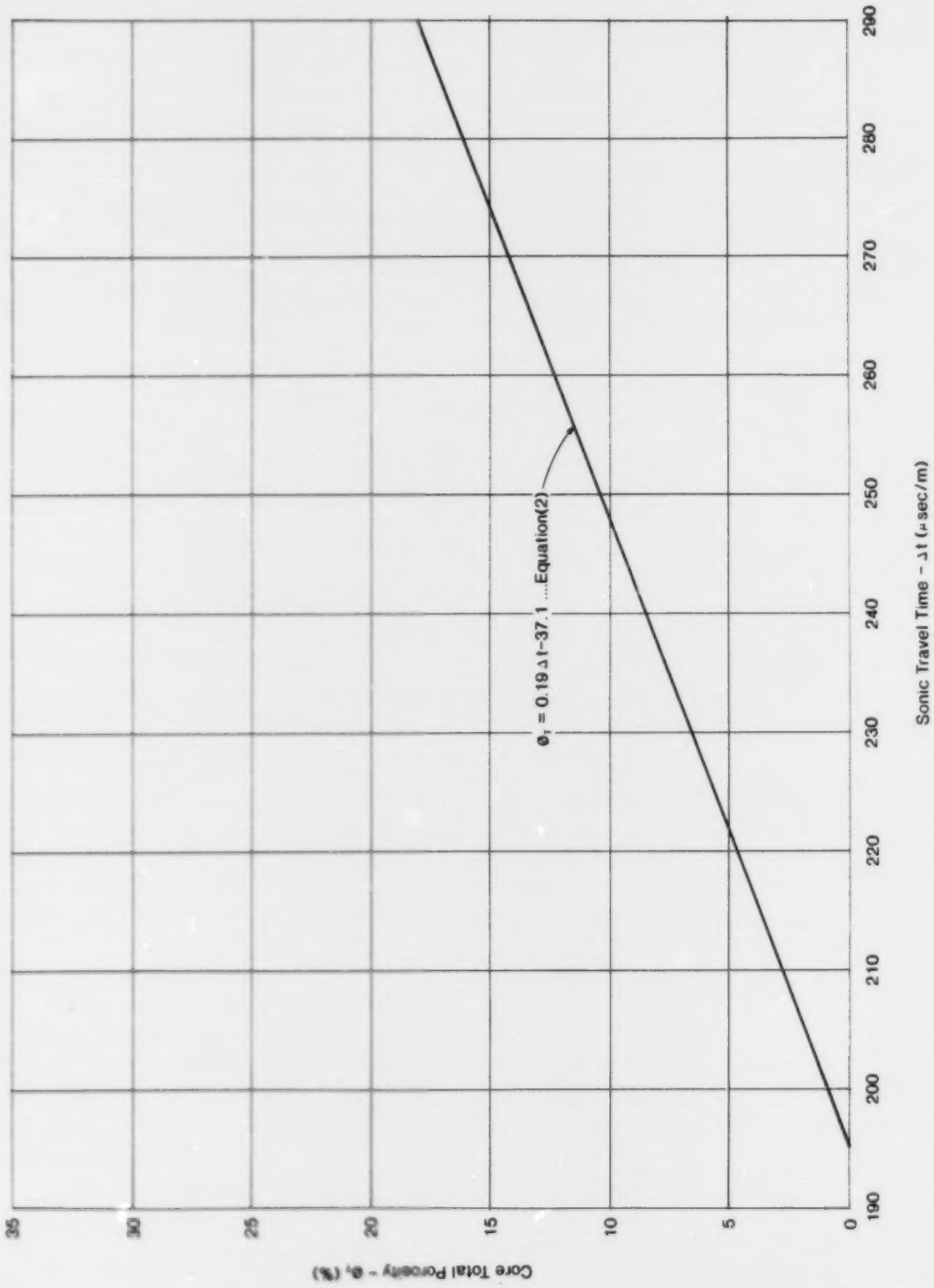

Figure 4: Core Total Porosity versus Sonic Travel Time

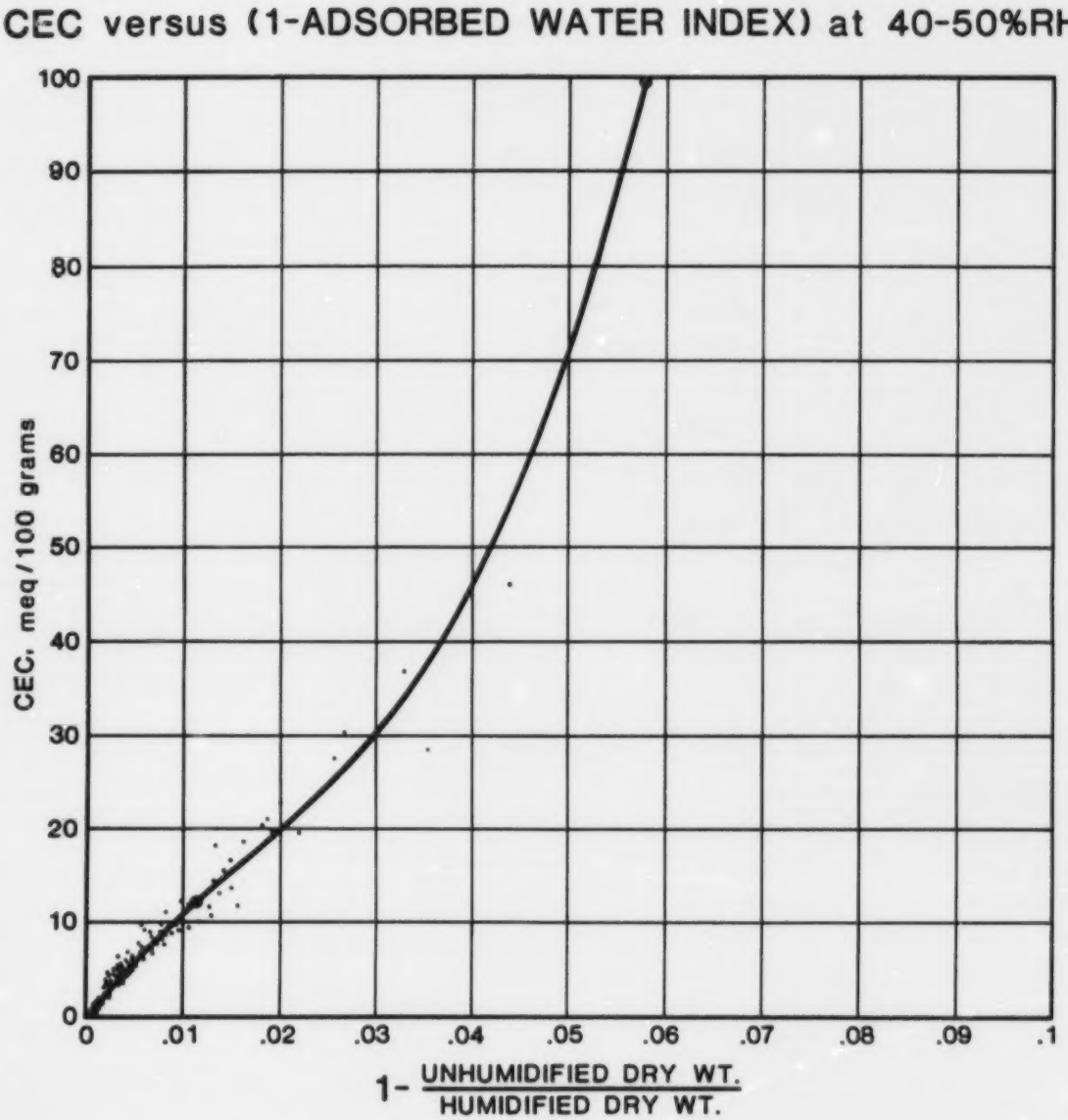

Figure 5: CEC versus(1-Adsorbed Water Index)

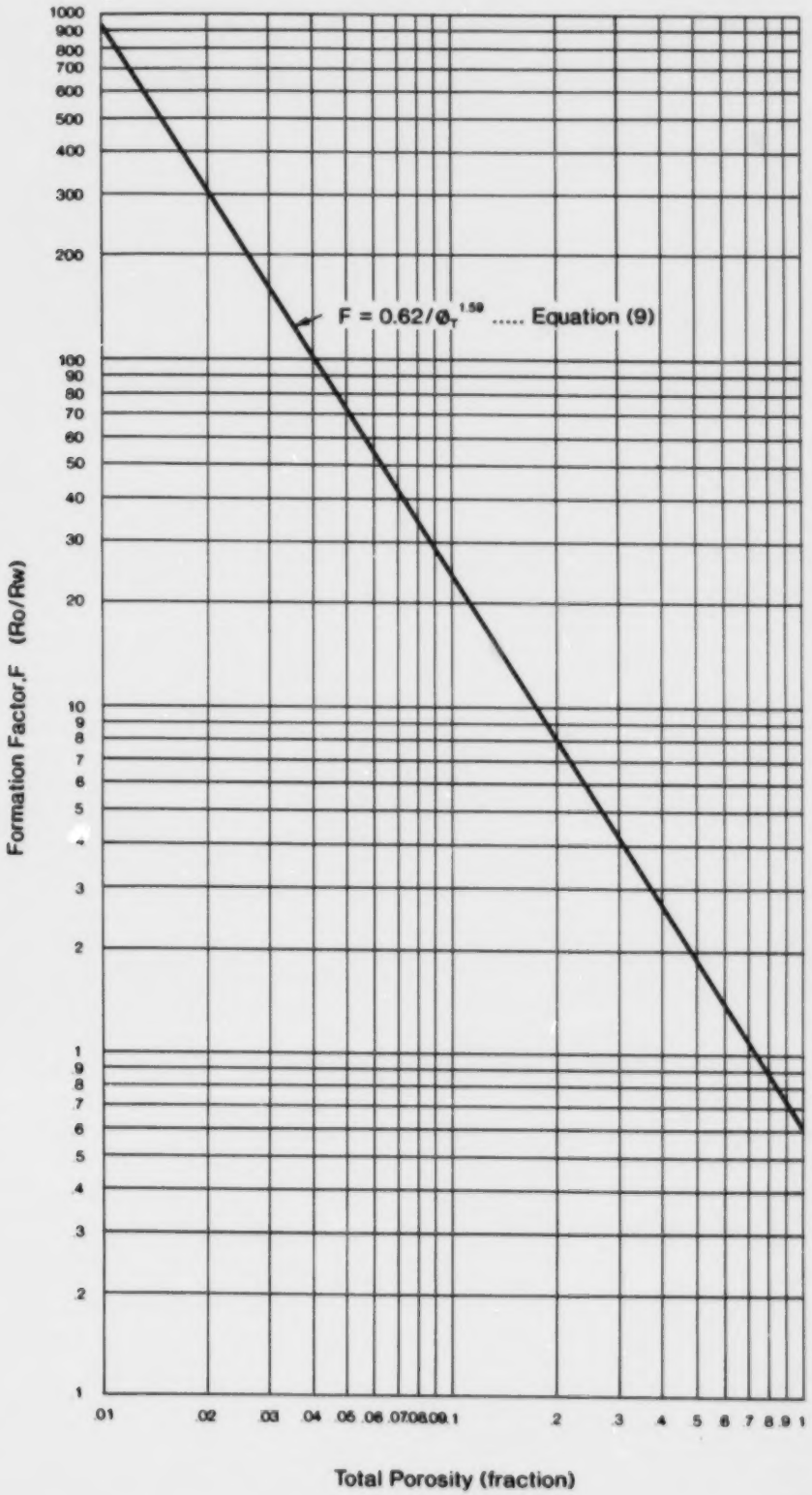

Figure 6: Formation Factor versus Total Porosity

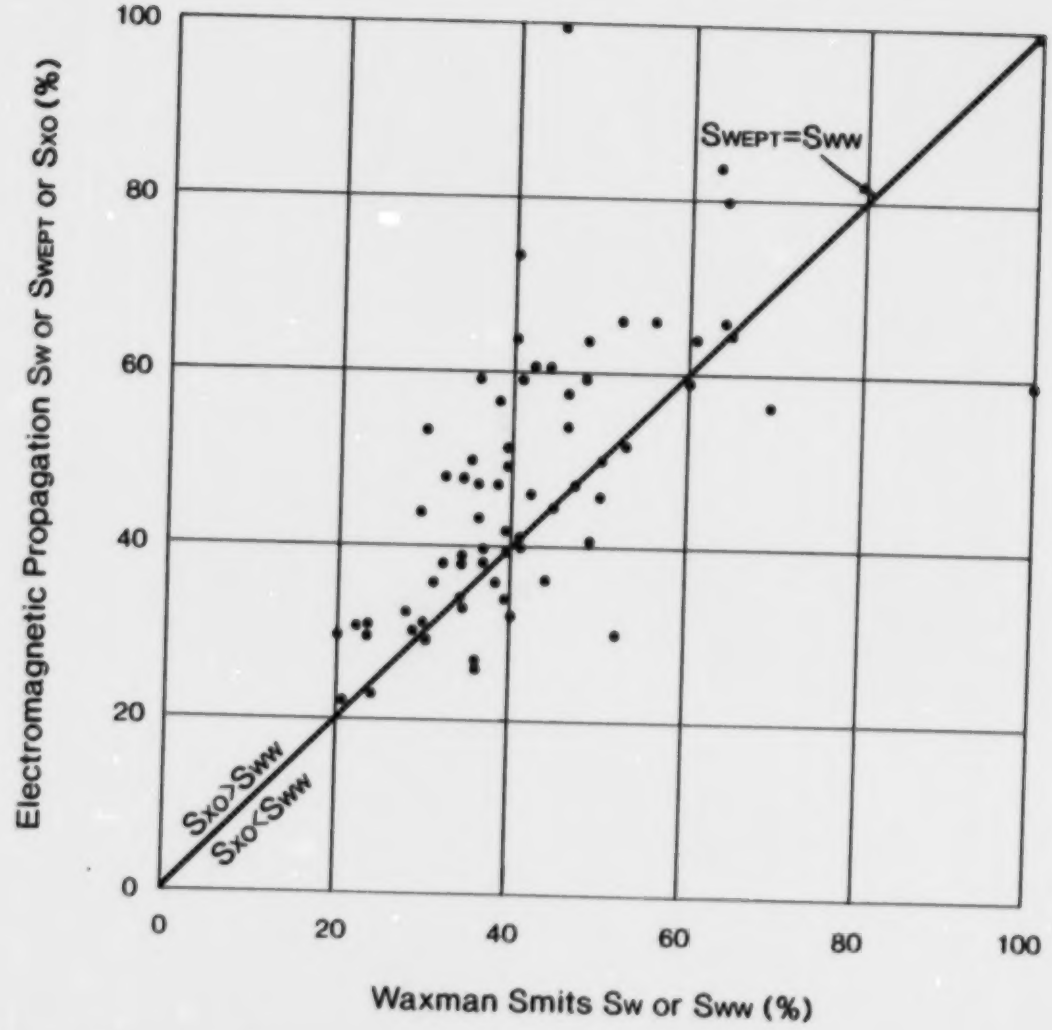

Figure 7: SWEPT versus Waxman-Smits Sw

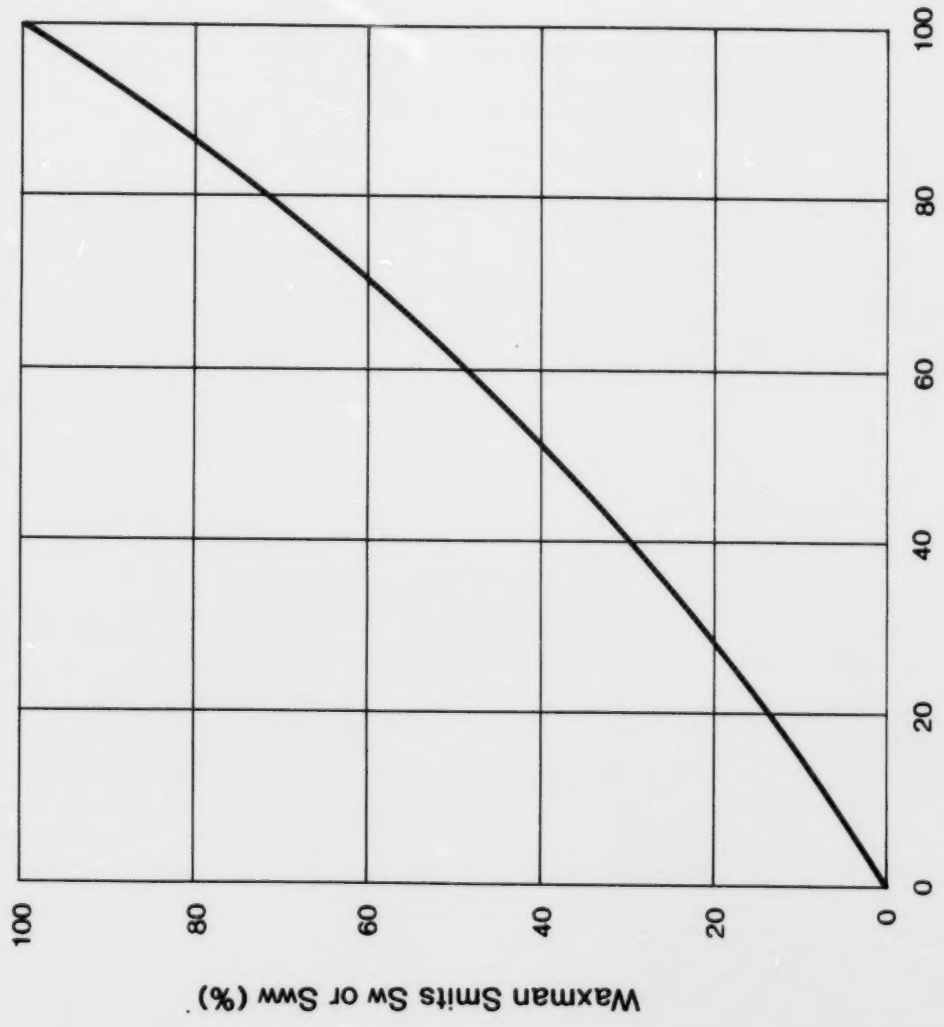

Figure 8: Waxman-Smits Sw versus Archie Sw

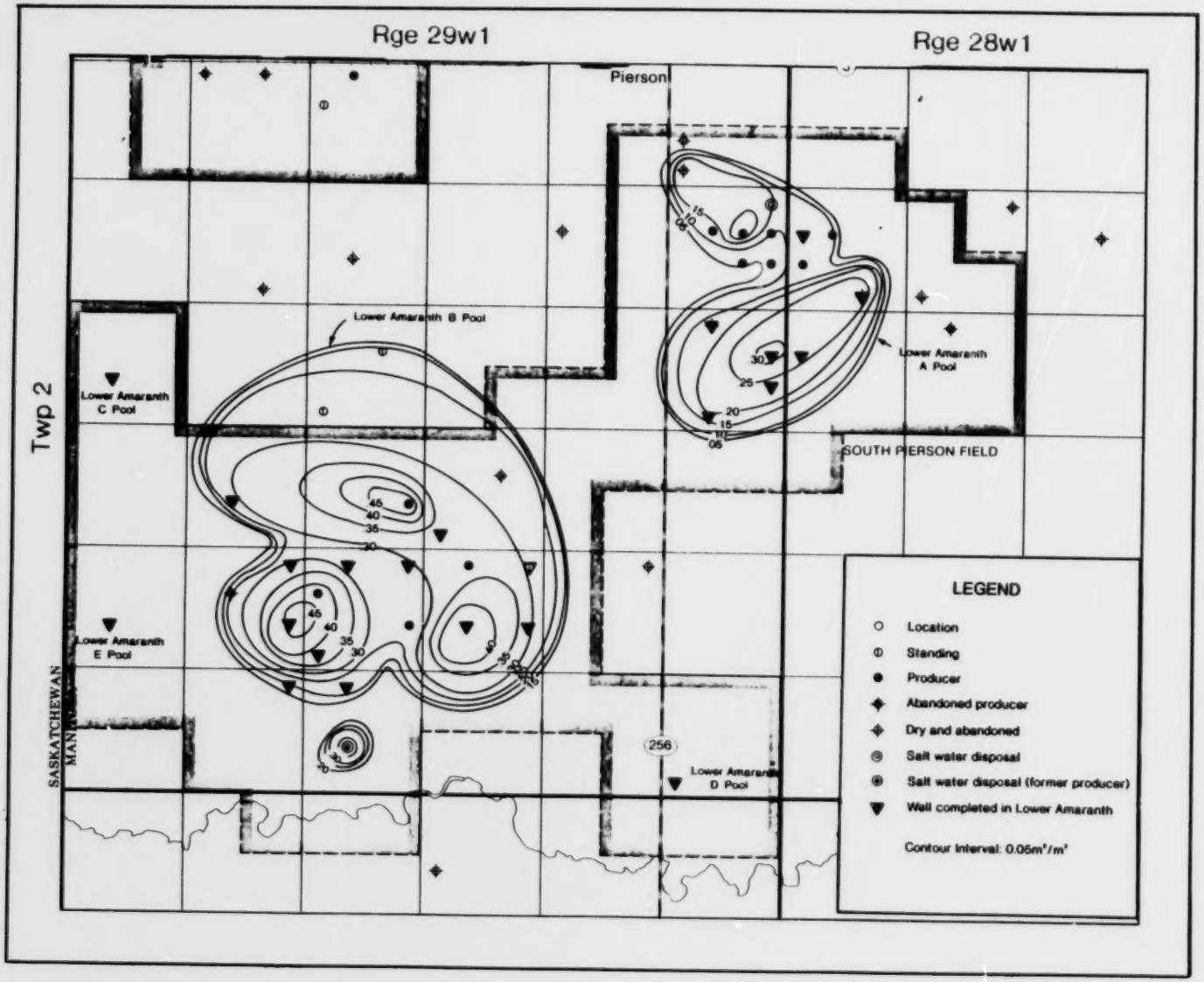

Figure 9: Lower Amaranth Formation South Pierson Field Original Oil-in-Place per Unit Area Map

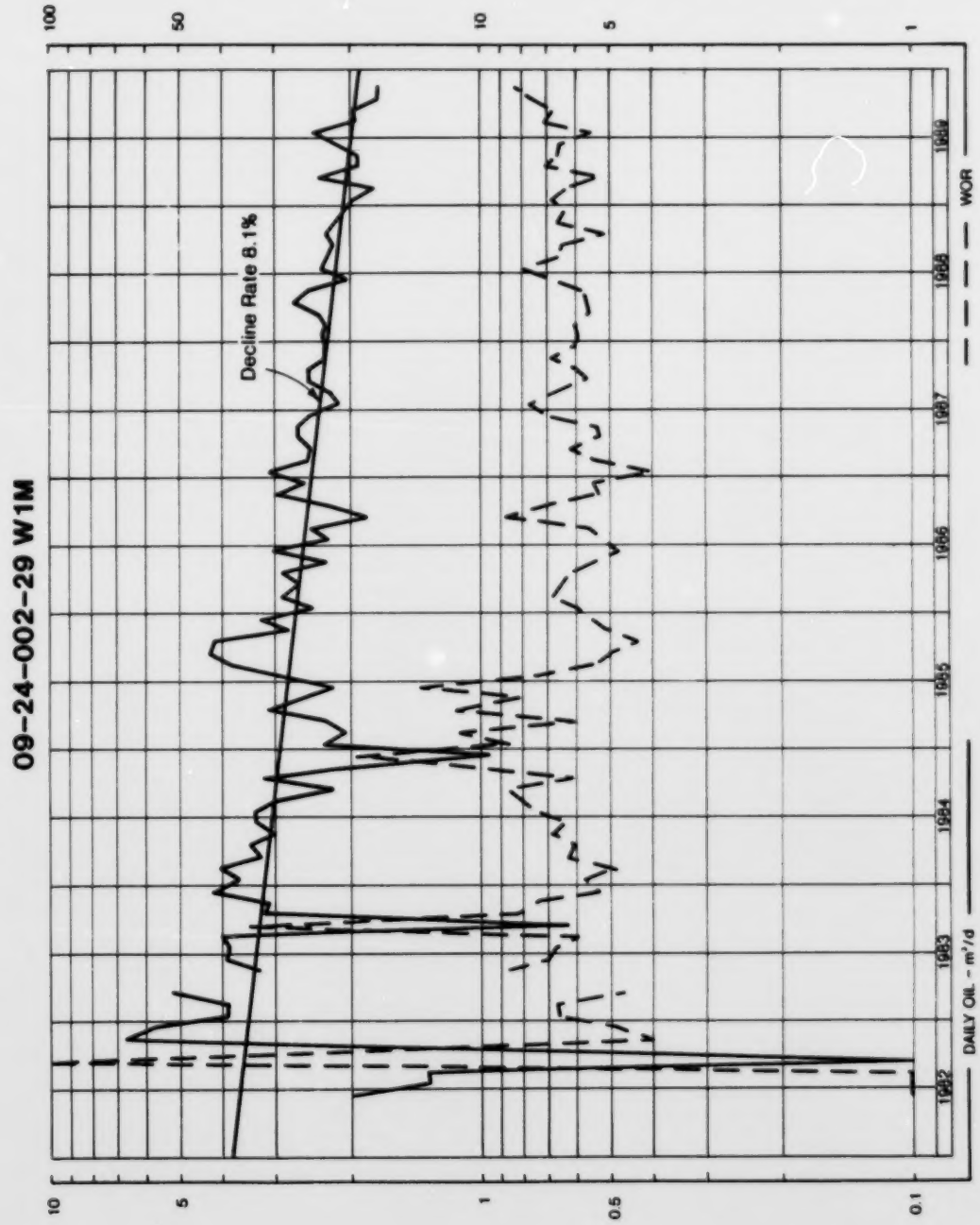

Figure 10: Production History for 9-24-2-29 WPM South Pierson Lower Amaranth A Pool

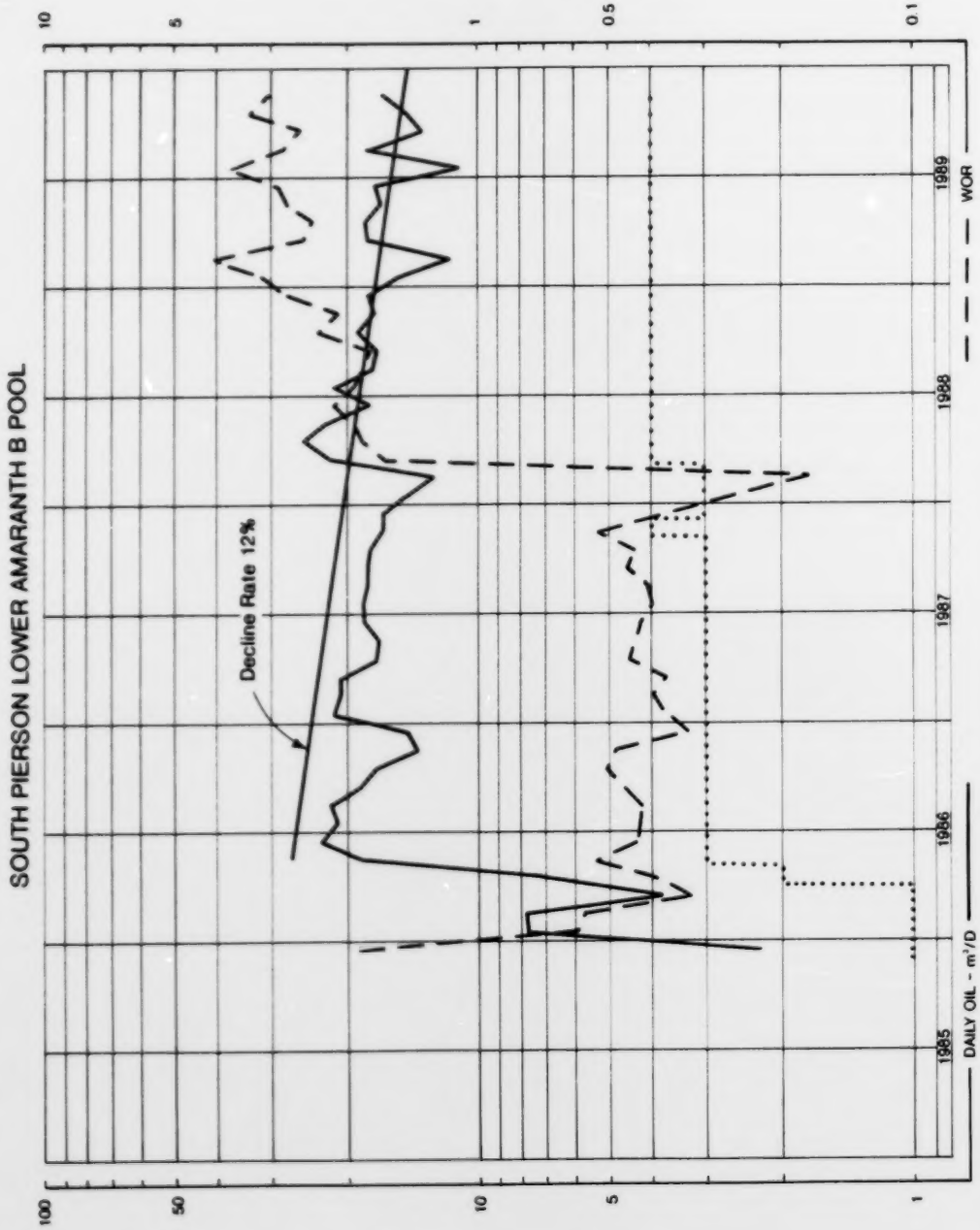

Figure 11: Production History for South Pierson Lower Amaranth B Pool (4 wells)

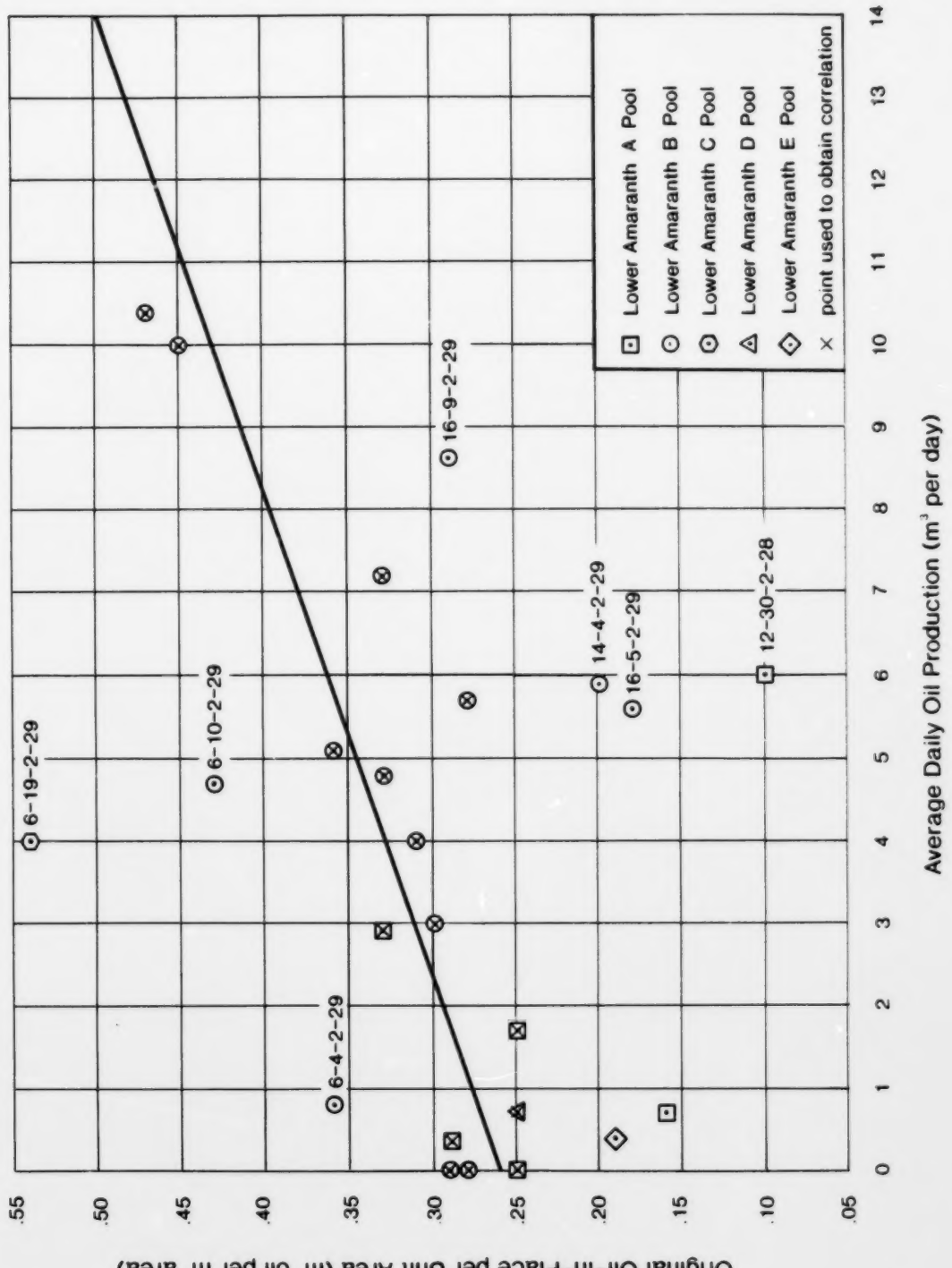

Figure 12: Original Oil-in-Place per Unit Area versus Oil Production

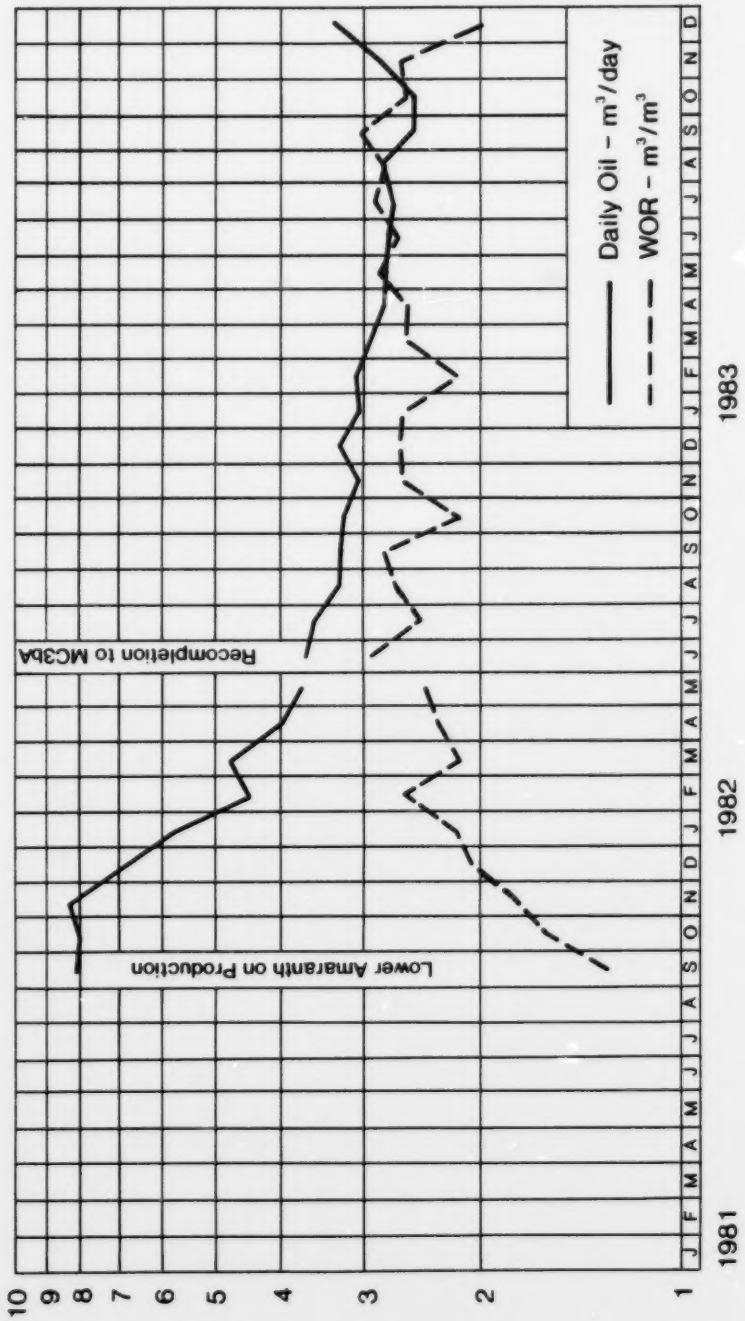

Figure 13: Production History for 12-30-2-28 WPM - South Pierson Lower Amaranth A Pool